creative commons
COMMONS DEED

저작자표시-비영리-변경금지 2.0 대한민국

이용자는 아래의 조건을 따르는 경우에 한하여 자유롭게

- 이 저작물을 복제, 배포, 전송, 전시, 공연 및 방송할 수 있습니다.

다음과 같은 조건을 따라야 합니다:

**저작자표시**. 귀하는 원저작자를 표시하여야 합니다.

**비영리**. 귀하는 이 저작물을 영리 목적으로 이용할 수 없습니다.

**변경금지**. 귀하는 이 저작물을 개작, 변형 또는 가공할 수 없습니다.

- 귀하는, 이 저작물의 재이용이나 배포의 경우, 이 저작물에 적용된 이용허락조건을 명확하게 나타내어야 합니다.
- 저작권자로부터 별도의 허가를 받으면 이러한 조건들은 적용되지 않습니다.

**저작권법에 따른 이용자의 권리는 위의 내용에 의하여 영향을 받지 않습니다.**

이것은 이용허락규약(Legal Code)을 이해하기 쉽게 요약한 것입니다.

Disclaimer

dCollection

Master's Thesis of Veterinary Biochemistry

# Hypermethylation of ANK2 on both Canine Mammary Tumors and Human Breast Cancer

## 개의 유선암과 인간의 유방암 모두에서의 ANK2 의 과 메틸화

2021 February

Graduate School of Veterinary Medicine

Seoul National University

Veterinary Biomedical Science Major

Johannes Josephus Schabort

# Hypermethylation of ANK2 on both Canine Mammary Tumors and Human Breast Cancer

Advisor: Professor Je-Yoel Cho

Submitting a master's thesis of
Veterinary Biochemistry

2020 November

Graduate School of Veterinary Medicine
Seoul National University
Veterinary Biomedical Science Major

Johannes Josephus Schabort

Confirming the master's thesis written by
Johannes Josephus Schabort
2020 December

Chair HANG LEE (Signature)

Vice Chair Je-Yoel Cho (Signature)

Examiner WAN HEE KIM (Signature)

# Abstract

Canine Mammary Tumors (CMT) constitute the most common tumor types found in female dogs. Understanding this cancer through extensive research is important not only for clinical veterinary applications, but also in the scope of comparative oncology. The use of DNA methylation as a biomarker has been noted for numerous cancers in the form of both tissue and liquid biopsies, yet the study of methylation in CMT has been limited. By analyzing our canine Methyl-binding domain sequencing (MBD-seq) data, we identified intron regions of canine ANK2 and EPAS1 as differentially methylated regions (DMGs) in CMT. Subsequently, we established quantitative Methylation Specific PCR (qMSP) of ANK2 and EPAS1 to validate the target hypermethylation in CMT tissue, as well as cell free DNA (cfDNA) from CMT plasma. Both ANK2 and EPAS1 were hypermethylated in CMT and highlighted as potential tissue biomarkers in CMT. ANK2 additionally showed significant hypermethylation in the plasma cfDNA of CMT, indicating that it could be a potential liquid biopsy biomarker as well. A similar trend towards hypermethylation was indicated in HBC at a specific CpG of

the ANK2 target on the orthologous human region, which validates the comparative approach using aberrant methylation in CMT.

**Keywords:** CMT; comparative oncology; hypermethylation; MSP; biomarker.

**Student Number:** 2019-25838

---

# Table of Contents

Abstract……3

Table of Contents……5

List of Figures and Tables……7

1. Introduction……9

2. Results……12

2.1Identification of differentially methylated region

2.2Evaluation of differentially methylated regions in CMT and adjacent normal tissue

2.3Detection of differential methylation in canine plasma cfDNA

2.4Orthologous human regions analyzed from TCGA data

3. Discussion……33

4. Materials and Methods……41

4.1Ethics

4.2Tissue and plasma samples

4.3Correlation analysis between methylation and gene expression

4.4DNA isolation

4.5Bisulfite Sequencing

4.6Quantitative Methylation-Specific PCR (qMSP)

4.7Human TCGA Data

Bibliography……53

# List of Figures and Tables

**Figure 1.** Selection of ANK2 and EPAS1 as CMT hypermethylated targets.

**Figure 2.** BSP Sequencing of ANK2 and EPAS1.

**Figure 3.** QMSP validation of ANK2 and EPAS1 hypermethylation.

**Figure 4.** CMT hypermethylation analysis in cfDNA.

**Figure 5.** Hypermethylation of orthologous human target ANK2 and EPAS1 regions.

**Table 1.** Sequence homology of target canine ANK2 and EPAS1 regions with their orthologous human regions.

**Table 2.** Orthologous ANK2 region in other species.

**Table 3.** Canine tissue and plasma information.

**Table 4.** Human female breast cancer and normal plasma samples.

Table 5. Primer sets for BSP and MSP.

# 1. Introduction

Canine Mammary Tumors (CMT) are the most common neoplasia diagnosed in female dogs and are found to be malignant in approximately 50% of cases [1-4]. Apart from the clear veterinary benefit to understanding the nature of this cancer more clearly, studying CMT can also be beneficial in the field of comparative oncology [5-7].

Dogs have been highlighted as excellent animal models for human cancer [5,6]; this includes the use of CMT as a comparative model for human breast cancer (HBC) [7-10]. The expedited study rate due to faster disease progression and shorter lifespan, histological and mechanistic similarities [5], spontaneous disease occurrence, and exposure to similar environments as humans make dogs ideal models for comparative oncology [11,12]. The similar environments to humans that dogs often inhabit as companion animals are particularly interesting from an epigenetic standpoint, as environmental stimuli have been known to influence epigenetics [13, 14].

DNA methylation is an important method of epigenetic regulation and thus has often been studied in relation to cancer [15]. Aberrant global hypomethylation and localized, specific hypermethylation of

tumor suppressors and hypomethylation of oncogenes are observed in cancer [16]. In CMT, aberrant methylation has been reported for a few genes such as ERα [17], DAPK1, MGMT [18], and BRCA1[19], yet gene-specific methylation of CMT remains largely unknown. These methylation changes are often observed early during carcinogenesis [20] making them ideal biomarkers for early detection and prognosis. Tissue biomarkers still remain the standard for cancer diagnosis and prognosis, yet in recent years the interest in liquid biopsy biomarkers have risen [21].

Liquid biopsies involve the investigation of cell-free DNA (cfDNA) found in the blood, plasma, serum, or other liquids from the body and often contain circulating tumor DNA. They are of clinical importance as they are less invasive and also allow for a more comprehensive view of the cancer biology as opposed to the view offered by tissue biopsies that is limited to a single site of the tumor at a single moment in the progression of the cancer [21]. Methylation of circulating cfDNA has been highlighted as a human cancer biomarker in liquid biopsies [22-24]. Previously, our lab has presented the cfDNA hypomethylation of LINE1 as a candidate liquid biopsy biomarker in both CMT and HBC, however, the method of restriction enzyme

digestion followed by quantitative-PCR needs to be improved further for clinical use [25].

This study set out to identify and investigate differentially methylated regions (DMRs) in CMT, initially validating our findings in CMT tissues and then also in cfDNA isolated from plasma obtained from dogs with CMT with the intent of establishing candidate tissue and liquid biomarkers for cfDNA. Additionally, we correlated our differentially methylated target regions in our CMT data with HBC data to see if the differential methylation seen in these diseases is consistent across species at the targeted sites.

# 2. Results

## 2.1. Identification of differentially methylated regions

Target hypermethylated DMRs were identified using MBD-seq and corresponding RNA-seq according to the scheme in Figure 1A. From our previous MBD-seq data obtained for 11 pairs of CMT and adjacent normal tissue from NCBI BioProject database (accession number PRJNA601533)[26], 16,061 differentially methylated genes (DMGs) were identified based on the presence of a differentially methylated region (DMR) within the gene body. To develop DNA methylation-based biomarkers applicable to CMT and HBC, we decided to narrow the scope to regions that contained a hypermethylated CpG island in CMT; a separate study could be performed to analyze the hypomethylated cohort. We further narrowed down the 1,269 hypermethylated DMGs, based on the fold change (log2 fold change >1.5). Of these 20 identified targets, EPAS1, ANK2, DST and RUSC2 indicated a downregulation of gene expression in CMT noted from the RNA-seq data. Of these, ANK2 and EPAS1 were at a significant level (p-value <0.05) and were thus selected for further analysis (Figure 1B). These identified CMT DMRs were found in CpG islands in the 21$^{st}$ and 1$^{st}$ introns of ANK2 and

EPAS1, respectively, and the increase in methylation in the cancer samples are shown via Linear Mixed Model (LMM) with thresholds of both 10% and 5% (Figure 1C). The overall methylation level detected via the MBD-seq for both target regions were shown to be significantly more methylated in the CMT samples as opposed to the normal samples (Figure 1D).

Of the 11 CMT/normal tissue pairs that were used for MBD-seq, 10 were also used in the RNA-seq analysis. These 10 pairs that had data for both MBD-seq and RNA-seq showed a general reverse correlation trend between expression and methylation for both targets, albeit not at a significant level (Figure 1E & F). Yet, the correlation plots and the associated density plots do clearly reveal that for both targets the level of methylation is higher in CMT than in normal, whereas the level of expression is lower. Compared to the paired normal samples an increase in methylation of ANK2 and EPAS1 along with a decrease in expression is indicated in 5/10 and 8/10 CMT samples, respectively (Figure 1E & F). Based on the accumulated bioinformatic data, comprising MBD-seq and RNA-seq data, ANK2 and EPAS1 were both highlighted as potential CMT biomarkers with

DMRs in CMT and were chosen as the targets for the remainder of this study.

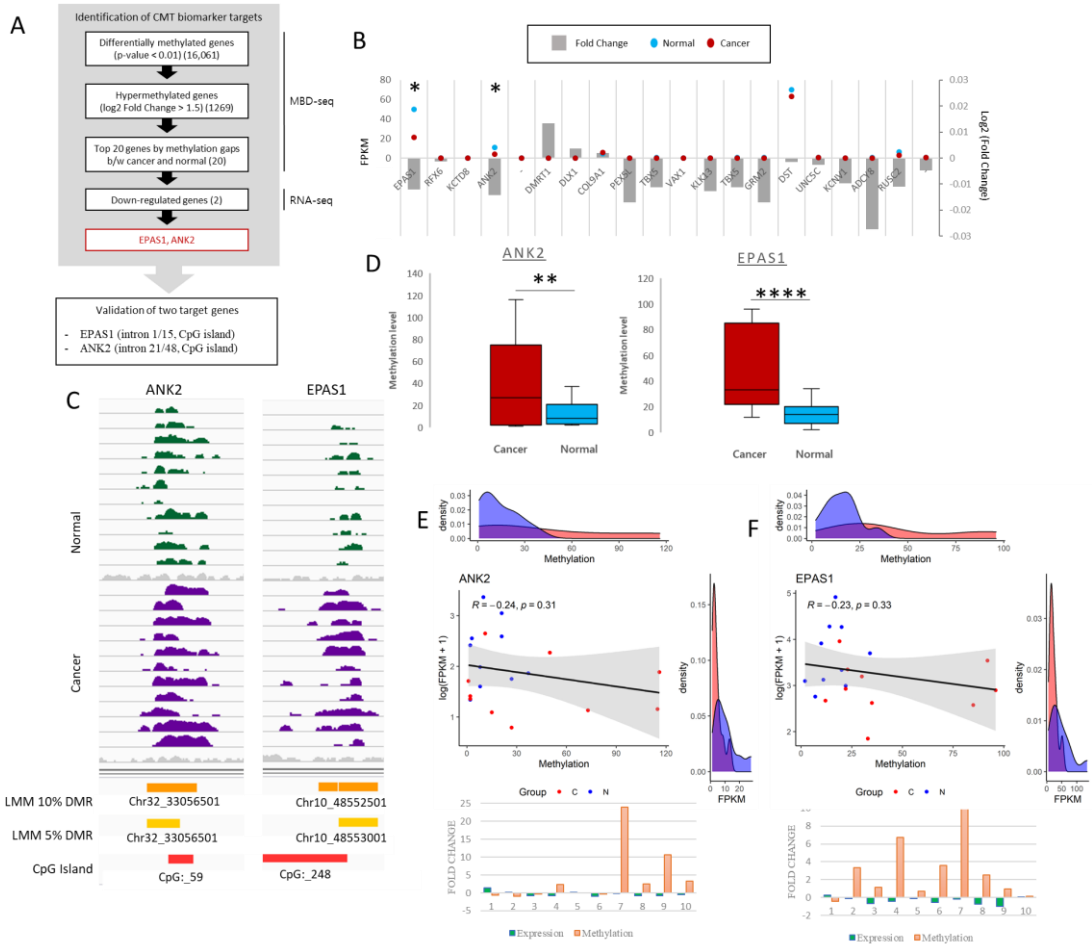


**Figure 1.** Selection of ANK2 and EPAS1 as CMT hypermethylated targets. (A) Schematic overview of target selection using MBD-seq and RNA-seq. (B) RNA-seq gene expression in FPKM of top 20 hypermethylated genes; blue dots=normal, red dots=CMT, * = p-value<0.05. Fold change (log2) for each target gene indicated with grey bar graph. (C) IGV peak calling for ANK2 and EPAS1 in both normal and cancer. Differential methylation assigned via LMM with both 5% and 10% threshold, and CpG island presence is indicated. (D)

Overall methylation levels of ANK2 and EPAS1 from MBD-seq data for 11 paired CMT and adjacent normal samples. EdgeR. ** = p.value<0.01, **** = <0.0001. (E) ANK2 and (F) EPAS1 correlation plots between expression (FPKM) and methylation of 10 paired CMT (red) and normal (blue) samples with matching density plots for both FPKM and methylation. Pearson correlation |r| value and p value indicated. Fold change graphs are also depicted for 10 CMT samples indicating expression (green) and methylation (orange).

## 2.2. Evaluation of differentially methylated regions in CMT and adjacent normal tissue

The target intron regions of ANK2 and EPAS1 that were identified through MBD-seq were further analyzed to assess their differential methylation. Quantitative Methylation Specific PCR (qMSP) was chosen as the method by which methylation was to be analyzed mainly due to its ability to quantify the methylation of numerous samples simultaneously without the need for exhaustive cloning and sequencing procedures. qMSP is furthermore a very sensitive technique that is able to distinguish a very small amount of methylated CpGs from unmethylated CpGs [27]. Sequencing was however still performed on three randomly selected pairs of CMT and normal gDNA for each target to establish a representative methylation pattern for each target and thus indicate in which areas to design the MSP primers (Figure 2). Both the ANK2 and EPAS1 target regions were methylated more in the CMT than the paired normal samples, although the amount of differential methylation was varied across the sample pairs (Figure 2).

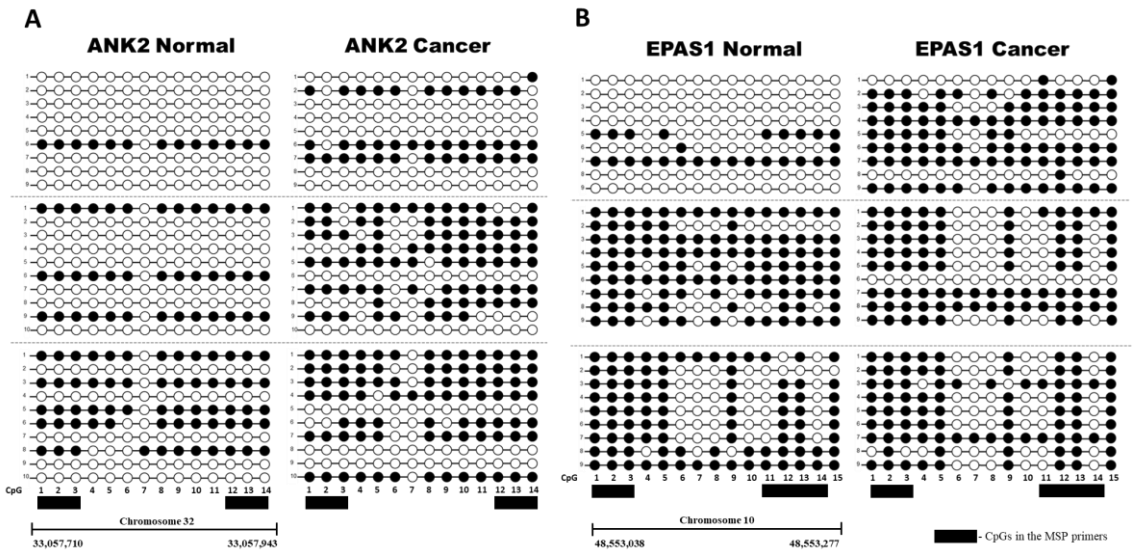


Figure 2. BSP Sequencing of ANK2 and EPAS1. Between 9 and 10 colonies were sequenced for three paired normal and CMT samples (separated by grey dotted line) for (A) ANK2 and (B) EPAS1. Methylation of a particular CpG is indicated by a black circle, and non-methylation is indicated by a white circle. The CpGs that were included in the forward and reverse MSP primers for each respective target with a black box.

qMSP was then performed to investigate more sample pairs. The Methylation Index is presented and is based on the Demethylation Index first introduced by Akirav et.al [28], with the adjustment of measuring the amount of methylated DNA as opposed to unmethylated DNA. This method uses bisulfite sequencing PCR (BSP) primers that flank the MSP region of interest to normalize the MSP readings (Figure 3A). Of the 15 sample pairs analyzed for the ANK2 target, 12 were more methylated in CMT compared to normal based on the methylation index, whereas 9 out of 15 EPAS1 target samples were more methylated in CMT than in paired normal (Figure 3B). The overall methylation was shown to be significantly more methylated in CMT for both the ANK2 and EPAS1 targets, based on paired t-tests (Figure 3C). Receiver Operating Characteristic (ROC) curves were constructed for both targets to access the sensitivity and specificity of using CMT hypermethylation as biomarkers. ANK2 had an Area under the curve (AUC) of 0.764, and EPAS1 had an AUC of 0.733 (Figure 3D). Overall, the quantitative MSP results validated what was shown in the MBD and sequencing data; the targeted ANK2 intron 21 and EPAS1 intron 1 regions are hypermethylated in CMT and are candidate tissue biomarkers for this disease.

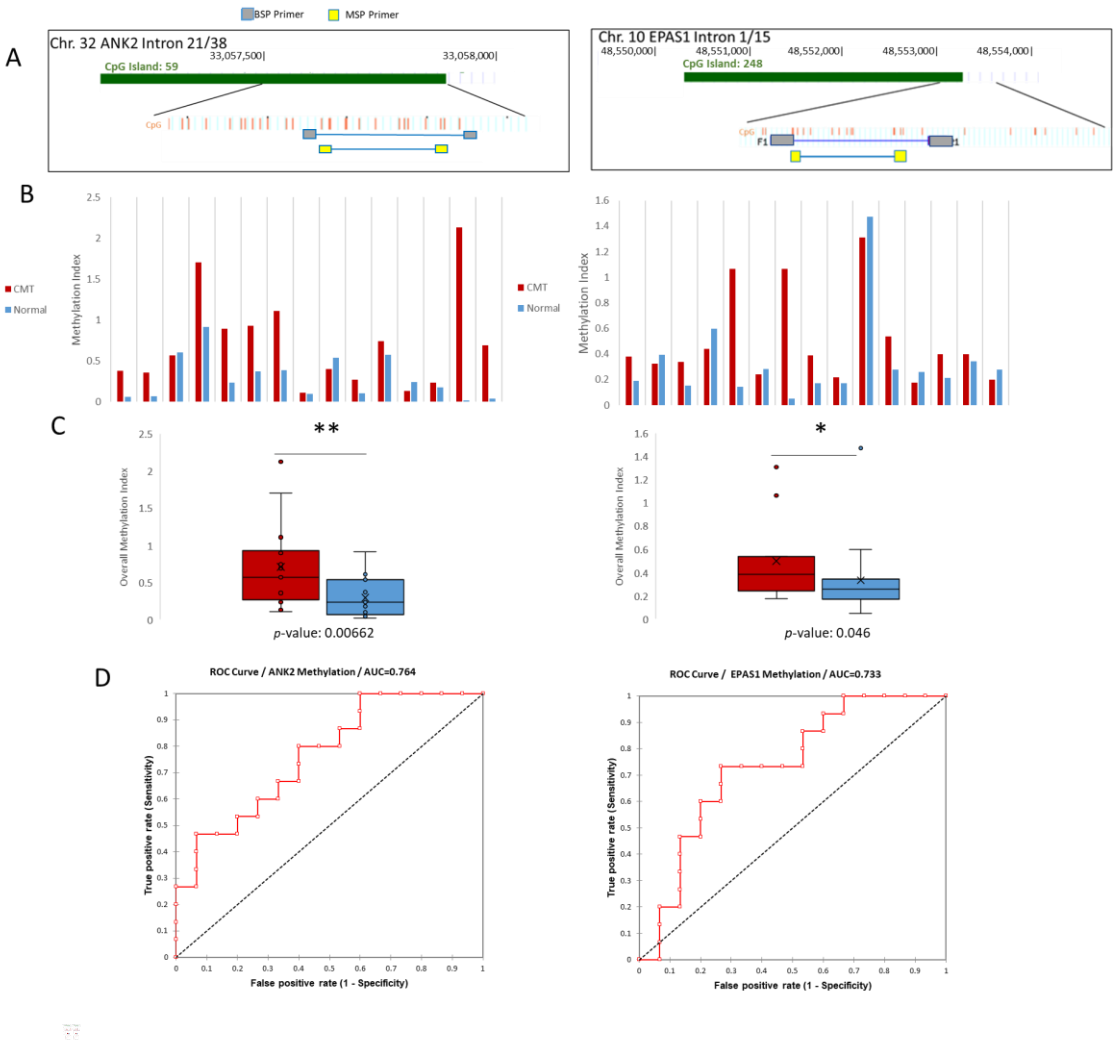


**Figure 3.** QMSP validation of ANK2 and EPAS1 hypermethylation. (A) Schemes for both ANK2 and EPAS1 indicating the target region in terms of its position on the CpG island of its respective intron. BSP primers (grey) are shown to flank the regions targeted by the MSP primers (yellow). (B) Methylation Indexes for both ANK2 and EPAS1. CMT samples are shown in red and paired

normal samples are shown in blue. (C) Overall methylation indexes for both ANK2 and EPAS1 are shown. CMT in red, normal in blue. * = p-value<0.05, ** = <0.01. (D) ROC curve analyses for ANK2 and EPAS1.

## 2.3 Detection of differential methylation in canine plasma cfDNA

qMSP has been utilized in previous studies to detect methylation of cfDNA [29,30]. One study found a significant agreement between ESR1 methylation of paired plasma and primary ovarian cancer tumors [31]. To evaluate whether the hypermethylation trends noted in CMT tissue could also be detected in cfDNA and thus serve as potential liquid biopsy biomarkers for CMT, we conducted the same qMSP procedure on cfDNA isolated from plasma samples of CMT and normal female dogs. The ANK2 target was analyzed in pooled cfDNA samples from 19 CMT dogs and 10 normal dogs. The hypermethylation trend of the ANK2 target region in CMT extended to cfDNA as is shown by the significantly higher methylation index (Fig 4A). Interestingly, the EPAS1 target, which was investigated in cfDNA samples from 10 CMT and 10 normal dogs, did not indicate an increased level of methylation for CMT as was seen in the tissue samples (Fig 4B). In contrast, the CMT cfDNA showed less methylation in CMT than normal plasma for EPAS1. Overall, in canine cfDNA, ANK2 demonstrated significant hypermethylation in CMT samples, which proposes it as a potential liquid biopsy biomarker for CMT.

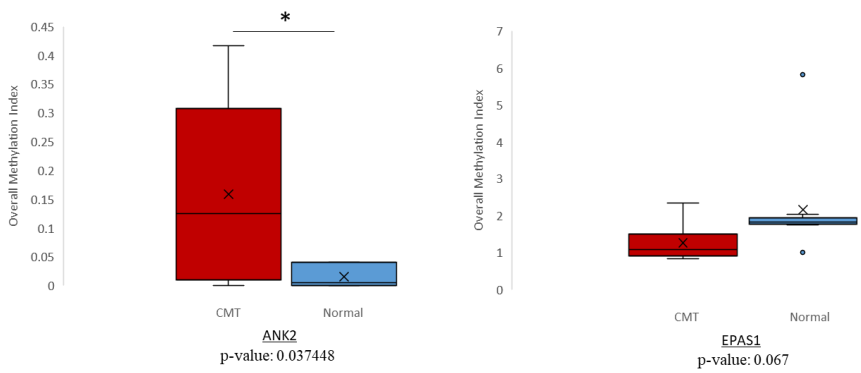


**Figure 4.** CMT hypermethylation analysis in cfDNA. Overall methylation index for (A) ANK2 and (B) EPAS1 in CMT (red) and normal (blue) cfDNA. * indicates p.value<0.05.

## 2.4. Orthologous human regions analyzed from TCGA data

To investigate whether the hypermethylation trend seen at the target regions in CMT would correspond to what is seen in HBC, we mapped the target regions found on the dog genome (CanFam3.1) to the human genome (HG19). This indicated that our 500 bp regions identified from the canine MBD-seq for the ANK2 and EPAS1 targets had orthologous human regions of 405 bp with 79% sequence identity and 221 bp with 76% sequence identity, respectively (Table 1). The EPAS1 target had an orthologous region that was also located in a CpG island at the 3' end of the first intron, just as in canines. The ANK2 target, which is situated in the 21$^{st}$ intron of the canine gene, similarly had an orthologous region in the 21$^{st}$ intron of human ANK2, however, this region does not contain a CpG island on the human genome, which makes it unsuitable for study with the qMSP method that we employed in this study. Even so, we investigated TCGA data for the target regions using Wanderer [32] and found ANK2 to be hypermethylated at 3 of the 4 CpG probes in this region (cg 25915539, cg17665652, and cg08448479), which corresponds to the hypermethylation that we observed in the orthologous region in dog (Fig 5A). Interestingly, even

though the amount of CpGs in this region is much less in humans than dogs, these three hypermethylated human CpGs are all conserved between the two species and were shown to be hypermethylated in the CMT dog samples (Fig 2A). The expression data from TCGA also indicated a downregulation of ANK2 in HBC, which matches our canine data (Fig 5B) and this data is further supported by the survival plot of ANK2 that shows a lower survival rate with decreased ANK2 expression (Fig 5C). The human EPAS1 region orthologous to the hypermethylated canine EPAS1 region that we analyzed contained 2 hypermethylated CpG probes according to the TCGA data (Fig 5D). Furthermore, the EPAS1 expression level was shown to be downregulated in HBC and the survival rate was decreased in accordance with EPAS1 downregulation (Fig 5E & F). The ANK2 target region, having been the better of the two targets, was furthermore investigated in additional species beyond canine and human. Mouse, rat, cat, and chimp all indicated orthologous intron regions with ≥74% identity conservation with the dog region (Table 2).

| | | % ID | Alignment length | Mismatches | Gaps open | e-value | bit-score |
|---|---|---|---|---|---|---|---|
| Canine ANK2 | Human ANK2 | | | | | | |
| chr32:33057501-33058000 | chr4:113292804-113293277 | 79.259 | 405 | 65 | 14 | 3.34E-75 | 265 |
| Canine EPAS1 | Human EPAS1 | | | | | | |
| chr10:48553001-48553500 | chr2:46299513-46300026 | 76.018 | 221 | 40 | 7 | 1.59E-37 | 141 |

Table 1. Sequence homology of target canine ANK2 and EPAS1 regions with their orthologous human regions.

| | Gene location | CpG Island | Regulatory Signatures | % ID | Alignment length | Gaps open | e-value | bit-score |
|---|---|---|---|---|---|---|---|---|
| Canine ANK2 | | | | | | | | |
| chr32:33057501-33058000 | Intron 21/48 | Yes | | | | | | |
| Human ANK2 | | | | | | | | |
| chr4:113292804-113293277 | Intron 19/43 | No | Proximal Enhancer-like | 79.259 | 405 | 14 | 3.34E-75 | 265 |
| Mouse ANK2 | | | | | | | | |
| chr3:126998115-126998598 | Intron 21/45 | No | Promotor-like | 74 | 423 | 26 | 3e-65 | 233 |
| Rat ANK2 | | | | | | | | |
| chr2:231301458-231301940 | Intron 19/21 | No | | 74 | 407 | 19 | 5e-63 | 224 |
| Cat ANK2 | | | | | | | | |
| chrB1:112372275-112372757 | Intron | Yes | | 82 | 501 | 19 | 3e-142 | 489 |
| Chimp ANK2 | | | | | | | | |
| chr4:110893204-110893679 | Intron | No | | 79 | 405 | 19 | 1e-95 | 334 |

Table 2. Orthologous ANK2 region in other species. Sequence homolgy information between dog and other species is indicated, along with the presence of CpG islands or other regulatory signatures.

To evaluate whether these trends would hold for clinical cfDNA samples, we isolated some from human plasma, obtained from both normal and HBC patients, and subjected it to bisulfite PCR sequencing. Unexpectedly, the EPAS1 target region did not show any methylation in this region for either HBC (4 samples) or normal (2 samples consisting of 5 and 6 pooled cfDNA isolates, respectively) (Data not shown), but this does coincide with the unexpected lack of cfDNA hypermethylation in CMT (Fig 4B). The hypermethylation trends shown in EPAS1 CMT tissue and HBC data from TCGA seems to not hold up in either canine or human cfDNA. On the other hand, sequencing results of the ANK2 target region from human cfDNA was more in line with what was suggested by the TCGA data. We sequenced colonies from 4 separate samples of HBC cfDNA and from 5 pooled normal cfDNA samples. Of the 3 CpGs indicated to be hypermethylated in this region from the TCGA data, only cg08448479, designated as CpG 5, was also shown to be more methylated in HBC cfDNA according to our sequencing results (Fig 5G). CpG 5 showed an increase in methylation from 71.88% in normal to 85.48% in HBC, which is consistent with the largest increase in methylation seen for the orthologous canine CpGs from 31.04% in normal to 62.07% in CMT (Fig 5G). We attempted to perform the qMSP procedure on pooled

samples of HBC cfDNA (14 samples) and pooled sample of normal human cfDNA (5 samples) with MSP primers that incorporated CpGs 1, 2, and 3 and CpGs 5 and 6 in the forward and reverse primers, respectively, but no significant difference was observed (Fig 5H). In both the TCGA dataset and the cfDNA sequencing, the ANK2 target indicated hypermethylation, even if limited to only a few CpGs, which is concurrent with what was seen in the canine CMT data.

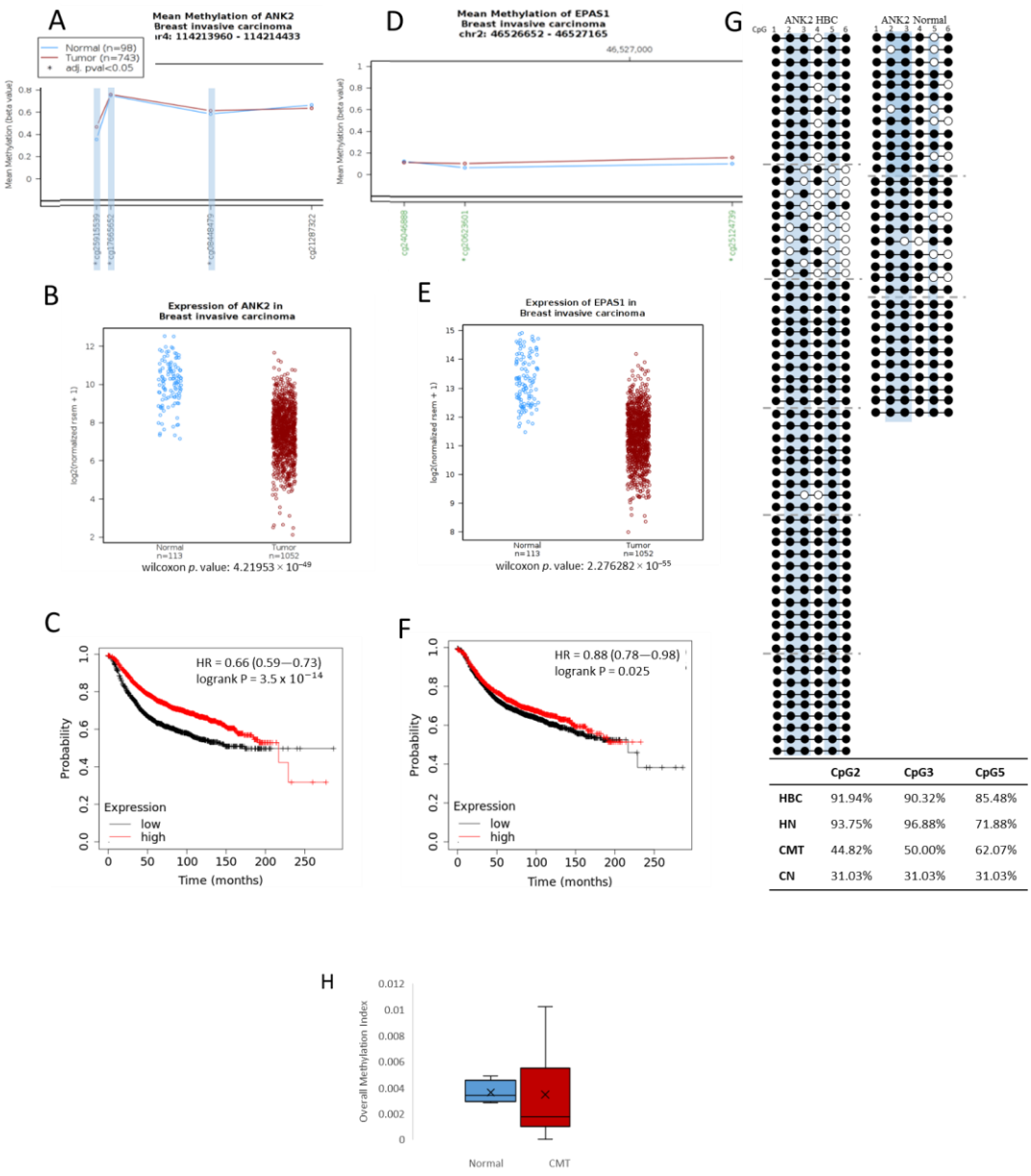


| | CpG2 | CpG3 | CpG5 |
|---|---|---|---|
| HBC | 91.94% | 90.32% | 85.48% |
| HN | 93.75% | 96.88% | 71.88% |
| CMT | 44.82% | 50.00% | 62.07% |
| CN | 31.03% | 31.03% | 31.03% |

**Figure 5.** Hypermethylation of orthologous human target ANK2 and EPAS1 regions. Mean Methylation (beta value) plots for orthologous human (A)ANK2 and (D)EPAS1 regions for normal

(blue) and invasive breast cancer patient(red) data obtained from TCGA. Specific methylation probes, annotated at the bottom of the graph are indicated to be in a CpG island when written in green ( only seen for EPAS1), and designated as significant (*) with an adjusted p-value <0.05. Three significantly hypermethylated CpGs from ANK2 are highlighted in light blue to indicate that they are conserved in the dog genome. (B) ANK2 and (E) EPAS1 log2 (normalized rsem + 1) expression data from TCGA for normal (blue) and invasive breast cancer patients (red). Wilcoxon p-values are indicated. (C) ANK2 and (F) EPAS1 Kaplan-Meier plots indicting relapse-free survival with high and low expressions each. (G) ANK2 sequencing results for cfDNA from normal and HBC patients. Between 10 and 11 colonies were sequenced for 6 individual HBC cfDNA samples (separated by grey dotted lines) and between 10 and 12 colonies were sequenced from 3 separate normal cfDNA samples. Methylation of a specific CpG is indicated by a black circle and non-methylation by a white circle. The CpGs at positions 2, 3, and 5 are highlighted in light blue as these are the CpGs that correlate with the hypermethylated CpG probes indicated in (A) and the respective percentage methylation for these CpGs in the HBC and

normal human (HN) cfDNA samples, as well as in canine CMT and normal (CN) tissue (Fig 2A), are indicated in the inserted table. (H) Overall Methylation Index for ANK2 in HBC and normal cfDNA.

# 3. Discussion

CMT is a common malignancy in female dogs and, moreover, in the scope of using dogs as animal models for human disease, its study can be translated to HBC. The field of comparative oncology using canine models have been increasing in popularity, yet the epigenome of canines with CMT remains incomplete. Methylation of DNA has been highlighted as a biomarker in both tissue and liquid biopsies [22-24] and thus we set out in this study to evaluate potential methylation biomarkers in CMT. This study identified novel regions in the 21$^{st}$ and 1$^{st}$ introns of ANK2 and EPAS1, respectively, that were significantly hypermethylated in CMT tissue and, in the case of ANK2, also in cfDNA isolated from dogs suffering from the disease. The ANK2 region was furthermore shown to be hypermethylated in human cfDNA at a corresponding CpG on the orthologous human region.

ANK2 encodes multiple AnkyrinB isoforms, which are integral membrane proteins that connect the lipid bilayer to the membrane skeleton [33]. In this present study, it was indicated that ANK2 mRNA expression was downregulated in CMT and also in HBC based on TCGA data. It is of note that other members of the ankyrin family, ANK1 and ANK3, have been shown to be overexpressed in multiple

human cancers including breast cancer [34,35], while ANK2 overexpression has been shown in pancreatic cancer where it contributed to the malignant phenotype [36]. However, other studies found that ANK2 gene expression was downregulated in colorectal cancer [37] and thyroid cancer [38], which corresponds to what we found in this study. The expression status and role of ANK2 seems to vary amongst cancer types, and further investigation in a larger variety of cancers is required to better understand its relationship to cancer. In cancers such as CMT and HBC, where ANK2 is downregulated, the role of its downregulation and the mechanisms by which its absence could aid in cancer progression remains unknown. Yet, knowing that the ANK2 protein is an integral membrane protein that connects the lipid bilayer to the membrane skeleton [33], it can be inferred that its downregulation would decrease the structural stability of the cell membrane making it more malleable. From this it can be hypothesized that the downregulation of ANK2 could promote the cancer phenotype by aiding in cellular dysplasia. The plasticity of the cellular membrane could further potentially promote metastasis by increasing cellular motility and migration as has been suggested with the downregulation of other membrane skeletal proteins [39-41]. Further study to confirm the role and mechanisms of downregulated

ANK2 in CMT and HBC is needed. Moreover, the role of cancer associated aberrant methylation in ANK2 remains largely unknown. One previous study compiled datasets for nasopharyngeal cancer and found ANK2 to be hypomethylated and upregulated, highlighting it as a potential biomarker for this cancer type [42]. Our study found a hypermethylated intron 21 region of ANK2, in both tissue and cfDNA, and it was highlighted as a potential tissue and liquid biopsy biomarker for CMT. Yet the impact of this specific methylation in CMT as well as the fuller extent of ANK2 methylation, on the promotor region for instance, remains unknown and should be studied further.

Of the other species that we investigated, cat showed the highest conservation of this ANK2 region at 82% identity and it was also the only other species that indicated a CpG island within this area suggesting that its regulation may be most similar, yet both human and mouse indicted regulatory signatures, which indicates this regions' potential importance in these species as well (Table 2). Unfortunately, of all these species, human is the only one with publicly available breast cancer/mammary gland cancer methylome data for this region. Mouse has some methylome data for this region, but not mammary gland specific and the only murine cancer methylome data is for colon

cancer, which did not show any differential methylation in this region. The orthologous human region does contain hypermethylated CpGs but outside of a CpG island which makes the qMSP method difficult, even more so when considering that of the 6 CpGs in the region only one seemed to be differentially methylated based on the sequencing data in Fig. 5G. The subsequent failure of the qMSP in distinguishing significantly between the HBC and Normal ANK2 is probably due to there only being 1 CpG (CpG 5) that is differentially methylated, and the technique is reliant on more than 1 CpG being differentially methylated. Additional sequencing of this region in more samples would be the best way to highlight the differential methylation in the respective CpGs. Other regions on ANK2 that contain conserved CpG islands could potentially be more successfully analyzed via the qMSP method and could potentially prove more influential in the downregulation of expression seen in Fig 5B. Pyrosequencing could be another alternative to pursue, as opposed to cloning and Sanger sequencing. We did not observe any methylation difference on the promoter region in our previous MBD-seq data [26]. This orthologous human region should be further studied in the future in tissue and cell culture to further investigate the nature and role of these hypermethylated CpGs play a significant role in HBC. To our

knowledge, no other study has yet to elucidate the state of ANK2 in either HBC or CMT, which makes our novel investigation of ANK2 in these diseases very insightful.

EPAS1, on the other hand, is relatively well studied in its relation to cancer, including breast cancer. EPAS1 is part of the Hypoxia Inducible Factor (HIF) family and plays an important role in the hypoxic response pathway which is often associated with tumorigenesis [43]. EPAS1 acts as a transcription factor in hypoxic conditions with many of its targets being known to contribute to carcinogenesis, such as VEGF and VEGF-R1 [43,44]. It has been highlighted as an oncogene in numerous cancer types [45, 46], however EPAS1 has also been described as tumor suppressive in various other cancer types including neuroblastoma, colon cancer, and hepatocellular carcinoma, and shown to reduce tumor growth and improve patient outcomes when overexpressed [47-50]. In breast cancer, the role and expression levels of EPAS1 have been indicated to be subtype specific. Klahan et. al [51] found EPAS1 to be a subtype specific lymphovascular invasion marker in ER- and HER2+ breast cancer. It has additionally been demonstrated that there is an estrogen dependent downregulation of EPAS1 in ER+ but not ER- HBC and

proposed EPAS1 as a negative prognostic marker in HER2 + invasive breast cancer, since overexpression of EPAS1 worsen the prognosis in HER2 and ER+ [52,53].

This present study indicated an overall downregulation of EPAS1 in CMT and in invasive HBC, yet the role of DNA methylation still remains unclear as, despite the indication of hypermethylation of the proposed region in the first intron of human EPAS1 shown in the TCGA data, the cfDNA analysis showed no methylation difference between normal and HBC patients. Similarly, the canine cfDNA data did not show any increased methylation in this region, however, significant hypermethylation was noted in CMT tissue compared to paired adjacent normal tissue. This discrepancy between the tissue methylation and cfDNA methylation could potentially be explained by a lesser abundance of circulating tumor DNA (ctDNA) compared to normal cfDNA isolated from the plasma samples used, seeing as even though tumors usually secrete for a larger amount of cfDNA in the plasma there is currently no ideal method for separating ctDNA from total cfDNA. ctDNA is furthermore highly fragmented which could hinder its detection [54]. Analyzing the methylation of the EPAS1 target region in circulating tumor cells (CTCs) could prove insightful. The hypermethylation and mRNA downregulation noted in the CMT

tissue is however concurrent with previous studies where EPAS1 has been shown to be hypermethylated in its promotor with downregulated mRNA expression in non-small cell lung cancer [55] and colon cancer [49]. Although a separate study showed EPAS1 to be hypomethylated in colon cancer [56]. In CMT tissue, our study of EPAS1 and its indications of hypermethylation in cancer as opposed to normal remains a novel and intriguing finding and highlights this target as a candidate tissue biomarker for CMT. Yet, future studies should endeavor to delve deeper into the methylation of the targeted intron region in HBC by analyzing tissue and cell culture samples. Elucidating the functional role of this hypermethylation in CMT and potentially HBC, specifically in ER+ subtypes that have previously indicated downregulation in HBC [52] and in HER2 subtypes where it has been implicated as a prognostic marker [53], is important to understanding the regulation of EPAS1 and its potential role in CMT and HBC.

Overall, this study set out to investigate CMT tissues and cfDNA isolated from plasma obtained from dogs with CMT for potential biomarkers and attempt to translate the findings to HBC by ways of comparative oncology. This study identified novel hypermethylated intron regions for ANK2 and EPAS1 that could potentially serve as tissue biomarkers for CMT. Furthermore, the ANK2 target also

showed hypermethylation in cfDNA isolated from CMT, which highlights it as a potential liquid biopsy biomarker for CMT. In HBC 1 CpG from the orthologous human ANK2 region likewise indicated a hypermethylated trend in cfDNA isolated from HBC patients, which emphasizes the link between CMT and HBC epigenetic regulation.

# 4. Materials and Methods

## 4.1. Ethics

This study, including the materials and methods, was reviewed and approved by the Seoul National University Institutional Review Board/Institutional Animal Care and Use Committee (IACUC# SNU-170602-1/IRB#SNU 16-10-063), Samsung Medical Center IRB (#SMC2016-07-129-015), and the Seoul Metropolitan Government - Seoul National University Boramae Medical Center IRB (#20161123/16-2016-99/121).

## 4.2. Tissue and plasma samples

Tissue samples used in this study consisted of surgically removed CMT tissue and paired adjacent normal tissue obtained from a variety of dog breeds. Tumors identified as carcinomas were selected, yet the selection was not subtype specific (simple, complex, and ductal carcinomas) seeing as the MBD-seq data (accession number PRJNA601533) [26] did not show any subtype specific differences in methylation patterns for our targets. Canine blood samples were taken from dogs diagnosed with mammary carcinoma and normal samples were obtained from healthy dogs without cancer. A detailed roster of

the dogs used can be found in Table 3. Depending on the dog size, 2 to 4 mL of blood was collected in Vacuette EDTA tubes (Greiner Bio-One, Kremsmunster, Austria).

| Sample | Type | Age | Breed | Histological Type |
|---|---|---|---|---|
| 1 | CMT and Adjacent Normal Tissue | 10 | Great Pyrenese | Complex |
| 2 | CMT and Adjacent Normal Tissue | 13 | Cocker Spaniel | Ductal |
| 3 | CMT and Adjacent Normal Tissue | 13 | Cocker Spaniel | Tubular |
| 4 | CMT and Adjacent Normal Tissue | 13 | Schnauzer | Complex/Ductal |
| 5 | CMT and Adjacent Normal Tissue | 11 | Dachshund | Complex |
| 6 | CMT and Adjacent Normal Tissue | 15 | Poodle | Mixed |
| 7 | CMT and Adjacent Normal Tissue | 10 | Dachshund | Complex/Ductal |
| 8 | CMT and Adjacent Normal Tissue | 6 | Maltese | Unknown |
| 9 | CMT and Adjacent Normal Tissue | 14 | Shih-tzu | Mixed |
| 10 | CMT and Adjacent Normal Tissue | 14 | Schnauzer | Complex |
| 11 | CMT and Adjacent Normal Tissue | 14 | Schnauzer | Complex |
| 12 | CMT and Adjacent Normal Tissue | 11 | Maltese | Complex |
| 13 | CMT and Adjacent Normal Tissue | 13 | Cocker Spaniel | Simple |
| 14 | CMT and Adjacent Normal Tissue | 17 | Yorkshire Terrier | Complex |
| 15 | CMT and Adjacent Normal Tissue | 10 | Shih-tzu | Complex |
| 16 | CMT and Adjacent Normal Tissue | 16 | Schnauzer | Tubular |
| 17 | CMT and Adjacent Normal Tissue | 14 | Poodle | Unknown |
| 18 | CMT and Adjacent Normal Tissue | 10 | Shih-tzu | Unknown |
| 19 | CMT and Adjacent Normal Tissue | 14 | Dachshund | Adenocarcinoma |
| 20 | CMT and Adjacent Normal Tissue | 3 | Dachshund | Complex |
| 21 | CMT and Adjacent Normal Tissue | 12 | Shih-tzu | Simple |
| 22 | CMT and Adjacent Normal Tissue | 10 | Beagle | Ductal |
| 13 | CMT Plasma | 13 | Cocker Spaniel | Simple |
| 23 | CMT Plasma | 14 | Cocker Spaniel | Unknown |
| 24 | CMT Plasma | 13 | Korean Jindo | Adenocarcinoma |
| 25 | CMT Plasma | 11 | Maltese | Complex |
| 26 | CMT Plasma | 13 | Mixed | Complex |
| 27 | CMT Plasma | 13 | Yorkshire Terrier | Unknown |
| 28 | CMT Plasma | 14 | Dachshund | Complex |
| 29 | CMT Plasma | 5 | Poodle | Simple |
| 30 | CMT Plasma | 14 | Poodle | Complex |
| 31 | CMT Plasma | 12 | Bichon Frise | Complex |
| 32 | CMT Plasma | 11 | Cavalier King Charles Spaniel | Adenocarcinoma |
| 33 | CMT Plasma | 16 | Shih-tzu | Unknown |
| 34 | CMT Plasma | 14 | Cocker Spaniel | Unknown |
| 35 | CMT Plasma | 15 | Shih-tzu | Unknown |
| 36 | CMT Plasma | 14 | Mixed | Adenocarcinoma |
| 37 | CMT Plasma | 16 | Mixed | Complex |
| 38 | CMT Plasma | 8 | Alaskan Malamute | Unknown |
| 39 | CMT Plasma | 16 | Mixed | Adenocarcinoma |
| 40 | CMT Plasma | 14 | Poodle | Adenocarcinoma |
| 41 | Healthy Canine Plasma | 10 | Schnauzer | |
| 42 | Healthy Canine Plasma | 12 | Schnauzer | |
| 43 | Healthy Canine Plasma | 3 | Pomeranian | |
| 44 | Healthy Canine Plasma | 8 | Maltese | |
| 45 | Healthy Canine Plasma | 13 | Weimaraner | |
| 46 | Healthy Canine Plasma | 7 | Maltese | |
| 47 | Healthy Canine Plasma | 2 | Bichon Frise | |
| 48 | Healthy Canine Plasma | 8 | Poodle | |
| 49 | Healthy Canine Plasma | 3 | Spitz | |
| 50 | Healthy Canine Plasma | 3 | Mixed | |

Table 3. Canine Tissue and Plasma Information. The sample type, age, breed, and histological type of CMT is indicated.

Human blood samples were obtained from Samsung Medical Center, Seoul. After written informed consent was given, 4 to 6 mL of human blood was obtained from HBC patients scheduled to undergo surgery and from healthy control subjects that indicated no breast abnormalities upon examination. A detailed roster of the human subjects can be found in Table 4.

Both canine and human plasma samples were separated from the whole blood immediately after blood collection. An equal volume of Ficoll-Paque PLUS (GE Healthcare, Orsay, France) was added to each blood sample and centrifuged for 30 min, at 500 g, 18 °C without brake. Plasma was collected from the supernatant and stored at -80℃ until use.

| ID | Status | Age | Stage | ER | PR | HER2 |
|---|---|---|---|---|---|---|
| BC005 | HBC | 35 | IIA | + | + | - |
| BC012 | HBC | 36 | IIA | + | + | Equivocal |
| BC013P | HBC | 40 | IB | - | - | - |
| BC018 | HBC | 55 | 0 | - | - | + |
| BC016 | HBC | 47 | IA | - | - | - |
| BC022 | HBC | 54 | 0 | + | + | - |
| BC023 | HBC | 48 | IA | + | + | - |
| BC032 | HBC | 44 | IIB | - | - | - |
| BC035 | HBC | 34 | IA | - | - | - |
| BC038P | HBC | 41 | IA | + | + | - |
| BC043P | HBC | 47 | IA | + | + | - |
| BC055P | HBC | 43 | IA | + | + | - |
| BC058P | HBC | 54 | IA | - | - | - |
| BC059P | HBC | 38 | 0 | - | - | + |
| BC060P | HBC | 42 | IIB | - | - | - |
| BB012P | Healthy | 48 | | | | |
| BB026 | Healthy | 28 | | | | |
| BB027 | Healthy | 30 | | | | |
| BB041 | Healthy | 40 | | | | |
| BB043 | Healthy | 36 | | | | |

Table 4. Human female breast cancer and healthy plasma samples. Sample ID, status, and age are indicated for all samples. HBC samples also indicate cancer stage as well as the presence of ER, PR, and HER2.

## 4.3. Correlation analysis between methylation and gene expression

We performed an integrative analysis of MBD-seq (accession number PRJNA601533) [26] and RNA-seq data (SRA accession number: SRR8741587-SRR8741602) [25] from 8 overlapped tissue samples to identify canine mammary gland DNA methylation markers. We first selected DMRs which are located in a CpG island on the gene body and examined the correlation between DNA methylation and gene expression for each sample. To inspect the impact of DNA methylation on the local regulation of gene expression, the Pearson correlation (r) was calculated between the read count for DMRs located in CpG regions and the expression values of the corresponding genes. Log (fpkm+ 1) values were used to avoid taking log0 in the case of there being 0 counts. $|r| > 0.3$ and an adjusted p-value $< 0.05$ were set as the cutoffs for a significant correlation.

## 4.4. DNA isolation

Genomic DNA was isolated from 25mg samples of paired CMT and adjacent normal tissues using the DNEasy Blood & Tissue kit (Qiagen, Hilden, Germany) according to the manufacturer's protocol. The

recovered gDNA was quantified using a nanodrop spectrophotometer. Circulating cfDNA was isolated from both human (Normal and Breast Cancer patients) and canine (Normal and CMT patients) plasma samples using the QIAamp Circulating Nucleic Acid Kit (Qiagen, Hilden, Germany) according to the manufacturer's instructions. In short, 500 uL of plasma was brought up to 1mL with PBS and lysed with proteinase K and Buffer ACL before being bound, washed, and eluted from QIAamp mini columns on a vacuum manifold. Recovered cfDNA was quantified with a Qubit 3.0 Fluorometer using the Qubit HS dsDNA Assay (Invitrogen, Waltham, USA), according to the manufacturer's protocol.

## 4.5. Bisulfite Sequencing

DNA samples were Bisulfite treated using the EZ DNA Methylation-Lightning kit (Zymo Research, Irvine, USA), according to the manufacturer's instructions. Bisulfite treated DNA was quantified using the Qubit ssDNA Assay on the Qubit 3.0 Fluorometer (Invitrogen, Waltham, USA). Paired samples were brought to equal concentrations by diluting with water as appropriate before qMSP was performed.

Randomly selected samples of Bisulfite treated gDNA was sequenced to ascertain what the general methylation patterns are for both the ANK2 and EPAS1 targets in both CMT and normal tissue. Bisulfite Sequencing PCR (BSP) was conducted using the BSP primers (Table 5) and HotStart Taq DNA Polymerase (Bioneer, Daejeon, South Korea). Successful amplification was validated via gel electrophoresis on 2.0% Agarose gels. PCR amplicons were purified using the MEGAquick-spin Plus Total Fragment DNA Purification kit (Intron Biotechnology, Seongnam, South Korea) according to the manufacturer's protocol. The amplicons were then ligated into pGEM T-Easy vector (Promega, Madison, USA) and transformed into competent E. coli cells via heat-shock at 45℃ for 45s and plated on LB Agar plates that had been treated with Ampicillin, X-Gal, and IPTG to allow for Blue/White screening of colonies. White colonies were picked and sent for Sanger sequencing (Macrogen, Seoul, South Korea). cfDNA from human samples, HBC and normal, were similarly subjected to BSP sequencing.

| | | Forward primer | Reverse primer | Product size (bp) | Anealing Temperature (℃) |
|---|---|---|---|---|---|
| **Canine** | ANK2 BSP | TGAGTTTTTGTATAGTTGTAGTTAAAT | CTACTCTTCTAATAAAAAACACTTAAC | 235 | 60 |
| | ANK2 MSP | AATTTGTTATCGAGTTTTTCGCGG | CGCTTTAACCCTAAAATAATCGAACG | 185 | 66 |
| | EPAS1 BSP | AGAAAATAAAATTATAGTTAGTTTTTTTGA | AAACTTTTCCCTATTCCCAAAT | 240 | 60.5 |
| | EPAS1 MSP | AGTTAGTTTTTTTGAGCGCGTTGCGG | AACCCGACGCAAAACCGCGA | 172 | 70 |
| **Human** | ANK2 BSP | GAGTATAGTAAGGGAGTTGTTAGT | CCATCTACTACAAATAAAATATTACCAT | 198 | 61 |
| | ANK2 MSP | CGGTGTAATTAAACGAATTGGGATTTC | CTACAAATAAAATATTACCATCGAAAACACG | 149 | 68 |
| | EPAS1 BSP | GGGAGGGAATTTGTGTATTTTAT | ATTTTTCCCCTACTCCCAAA | 182 | 60.5 |

Table 5. Primer sets for BSP and MSP.

## 4.6. Quantitative Methylation-Specific PCR (qMSP)

To investigate the methylation of both cancer and normal gDNA and cfDNA, quantitative MSP was performed on each sample with MSP primers (Table 5) using the CFX96 Real-time PCR Detection System (Bio-Rad Laboratories, Hercules, USA). The same samples were also subjected to quantitative PCR using the BSP primers (Table 5), which were designed to flank the region of interest, to normalize the MSP readings and allow for the calculation of the Methylation Index, which was based on the demethylation index first introduced by Akirav et.al [27]. Each qMSP reaction contained 0.5units Hotstart Taq DNA Polymerase (Bioneer, Daejeon, South Korea), 0.625mM MgCl2, 0.2mM dNTPs, 0.5X SYBER Green (Life Technologies, Carlsbad, USA) and 10pmol each of forward and reverse primers in a 20uL total volume. For the gDNA samples, 5-30ng of template DNA was added, whereas 120-1200pg was added for the cfDNA samples. Each sample was run in triplicate using both the MSP and BSP primer sets and the thermal cycler conditions were as follows: 95℃ for 15min, denaturation at 95℃ for 30s, annealing at Annealing Temperature (Table 5) for 30s, elongation at 72℃ for 30s and final elongation at 72℃ for 5min.

All primers were manually designed and checked using the OligoEvaluator™ webtool. MSP primers were designed with at least 6

CpGs included in the set of primers, and with at least one CpG located in the last 3 bases at the 3' ends of the primer. BSP primers were designed with at least 4 non-CpG C's included in the primer set. For canine primer optimization, there are not any universally methylated and unmethylated controls commercially available. In-house controls were thus made. In short, fully methylated canine controls were made by treating ~1ug of canine gDNA with MssI methyltransferase (New England Biolabs, Ipswich, USA) according to the manufacturer's protocol. Fully unmethylated DNA was made by performing PCR with primers that flank the region of interest. The resulting amplimers were thus devoid of any methylation and served as completely unmethylated control template. Human primers were optimized on fully methylated and fully unmethylated human HCT116 DKO DNA (Zymo Research, Irvine, USA).

## 4.7. Orthologous Species Data

Using liftOver [57], we were able to convert the canine (CanFam3.1) genome coordinates of the differentially methylated intron regions of ANK2 and EPAS1 that we identified from the MBD-seq data to their orthologous regions on the human (Hg38) mouse (mm10), rat (rn6), cat (felCAT8), and chimp (panTRO6)

genomes. BLAST (https://blast.ncbi.nlm.nih.gov) was used to align the nucleotide sequences and determine the amount of sequence homology.

HBC data for the ANK2 and EPAS1 intron targets was obtained using Wanderer [32], which utilizes 450k Infinium Chip methylation arrays and Illumina HISeq RNA-seq data from The Cancer Genome Atlas (TCGA). Survival plots were generated using Kaplan-Meier Plotter with the auto selected cutoff enabled, which utilizes the expression data for the genes of interest, ANK2 (202920_at) and EPAS1 (200878_at), and the relapse free survival data of 3951 patients obtained from the GEO database [58]. The Kaplan-Meier Plotter software groups expression into high or low according to the median expression and then uses a Kaplan-Meier Plot to compare the two groups [58].

# Bibliography


1. Moe L. Population-based incidence of mammary tumours in some dog breeds. *J Reprod Fertil Suppl*. 2001;57:439-443.
2. Sorenmo K. Canine mammary gland tumors. *Vet Clin North Am Small Anim Pract*. 2003;33(3):573-596. doi:10.1016/s0195-5616(03)00020-2
3. Salas Y, Márquez A, Diaz D, Romero L. Epidemiological Study of Mammary Tumors in Female Dogs Diagnosed during the Period 2002-2012: A Growing Animal Health Problem. *PLoS One*. 2015;10(5):e0127381. Published 2015 May 18. doi:10.1371/journal.pone.0127381
4. Sleeckx N, de Rooster H, Veldhuis Kroeze EJ, Van Ginneken C, Van Brantegem L. Canine mammary tumours, an overview. *Reprod Domest Anim*. 2011;46(6):1112-1131. doi:10.1111/j.1439-0531.2011.01816.x
5. Paoloni M, Khanna C. Translation of new cancer treatments from pet dogs to humans. *Nat Rev Cancer*. 2008;8(2):147-56.
6. Rowell JL, McCarthy DO, Alvarez CE. Dog models of naturally occurring cancer. Trends Mol Med. 2011;17(7):380-388. doi:10.1016/j.molmed.2011.02.004

7. Gray M, Meehan J, Martínez-Pérez C, et al. Naturally-Occurring Canine Mammary Tumors as a Translational Model for Human Breast Cancer. *Front Oncol*. 2020;10:617. Published 2020 Apr 28. doi:10.3389/fonc.2020.00617
8. Strandberg JD, Goodman DG. Animal model of human disease: canine mammary neoplasia. *Am J Pathol*. 1974;75(1):225-228.
9. Visan S, Balacescu O, Berindan-Neagoe I, Catoi C. In vitro comparative models for canine and human breast cancers. *Clujul Med*. 2016;89(1):38-49. doi:10.15386/cjmed-519
10. Abdelmegeed SM, Mohammed S. Canine mammary tumors as a model for human disease. *Oncol Lett*. 2018;15(6):8195-8205. doi:10.3892/ol.2018.8411
11. Bukowski JA, Wartenberg D, Goldschmidt M. Environmental causes for sinonasal cancers in pet dogs, and their usefulness as sentinels of indoor cancer risk. *J Toxicol Environ Health A*. 1998;54(7):579-591. doi:10.1080/009841098158719
12. Lin CH, Lo PY, Wu HD, Chang C, Wang LC. Association between indoor air pollution and respiratory disease in companion dogs and cats. *J Vet Intern Med*. 2018;32(3):1259-1267. doi:10.1111/jvim.15143

13. Bollati V, Baccarelli A. Environmental epigenetics. Heredity (Edinb). 2010 Jul;105(1):105-12. doi: 10.1038/hdy.2010.2. Epub 2010 Feb 24. PMID: 20179736; PMCID: PMC3133724.

14. Baccarelli A, Bollati V. Epigenetics and environmental chemicals. Curr Opin Pediatr. 2009 Apr;21(2):243-51. doi: 10.1097/mop.0b013e32832925cc. PMID: 19663042; PMCID: PMC3035853.

15. Pfeifer GP. Defining Driver DNA Methylation Changes in Human Cancer. *Int J Mol Sci*. 2018;19(4):1166. Published 2018 Apr 12. doi:10.3390/ijms19041166

16. Baylin SB, Jones PA. Epigenetic Determinants of Cancer. *Cold Spring Harb Perspect Biol*. 2016;8(9):a019505. Published 2016 Sep 1. doi:10.1101/cshperspect.a019505

17. Brandão YO, Toledo MB, Chequin A, et al. DNA Methylation Status of the Estrogen Receptor α Gene in Canine Mammary Tumors. *Vet Pathol*. 2018;55(4):510-516. doi:10.1177/0300985818763711

18. Ren X, Li H, Song X, Wu Y, Liu Y. 5-Azacytidine treatment induces demethylation of *DAPK1* and *MGMT* genes and inhibits growth in canine mammary gland tumor cells. *Onco Targets Ther*.

2018;11:2805-2813. Published 2018 May 15.
doi:10.2147/OTT.S162381

19. Qiu H, Lin D. Roles of DNA mutation in the coding region and DNA methylation in the 5' flanking region of BRCA1 in canine mammary tumors. *J Vet Med Sci*. 2016;78(6):943-949.
doi:10.1292/jvms.15-0557

20. Feinberg, A., Ohlsson, R. & Henikoff, S. The epigenetic progenitor origin of human cancer. *Nat Rev Genet.* 2006;**7**:21-33.
doi:10.1038/nrg1748

21. Perakis S, Speicher MR. Emerging concepts in liquid biopsies. *BMC Med*. 2017;15(1):75. Published 2017 Apr 6.
doi:10.1186/s12916-017-0840-6

22. Board, R. E., Knight, L., Greystoke, A., Blackhall, F. H., Hughes, A., Dive, C., & Ranson, M. DNA Methylation in Circulating Tumour DNA as a Biomarker for Cancer. *Biomarker Insights*. 2007
doi:10.1177/117727190700200003

23. Huang J, Wang L. Cell-Free DNA Methylation Profiling Analysis-Technologies and Bioinformatics. *Cancers (Basel)*. 2019;11(11):1741. Published 2019 Nov 6.
doi:10.3390/cancers11111741

24. Constâncio V, Nunes SP, Henrique R, Jerónimo C. DNA Methylation-Based Testing in Liquid Biopsies as Detection and Prognostic Biomarkers for the Four Major Cancer Types. *Cells*. 2020;9(3):624. Published 2020 Mar 5. doi:10.3390/cells9030624

25. Lee KH, Shin TJ, Kim WH, Cho JY. Methylation of LINE-1 in cell-free DNA serves as a liquid biopsy biomarker for human breast cancers and dog mammary tumors [published correction appears in Sci Rep. 2019 Nov 20;9(1):17459]. *Sci Rep*. 2019;9(1):175. Published 2019 Jan 17. doi:10.1038/s41598-018-36470-5

26. Nam, A., Lee, K., Hwang, H. *et al.* Alternative methylation of intron motifs is associated with cancer-related gene expression in both canine mammary tumor and human breast cancer. *Clin Epigenet.* 2020;12:110. doi10.1186/s13148-020-00888-4

27. Herman JG, Graff JR, Myöhänen S, Nelkin BD, Baylin SB. Methylation-specific PCR: a novel PCR assay for methylation status of CpG islands. *Proc Natl Acad Sci U S A*. 1996;93(18):9821-9826. doi:10.1073/pnas.93.18.9821

28. Akirav EM, Lebastchi J, Galvan EM, et al. Detection of β cell death in diabetes using differentially methylated circulating DNA. *Proc*

*Natl Acad Sci U S A*. 2011;108(47):19018-19023. doi:10.1073/pnas.1111008108

29. Eissa MAL, Lerner L, Abdelfatah E, et al. Promoter methylation of ADAMTS1 and BNC1 as potential biomarkers for early detection of pancreatic cancer in blood. *Clin Epigenetics*. 2019;11(1):59. Published 2019 Apr 5. doi:10.1186/s13148-019-0650-0
30. Giannopoulou L, Mastoraki S, Buderath P, et al. ESR1 methylation in primary tumors and paired circulating tumor DNA of patients with high-grade serous ovarian cancer. *Gynecol Oncol*. 2018;150(2):355-360. doi:10.1016/j.ygyno.2018.05.026
31. Giannopoulou L, Chebouti I, Pavlakis K, Kasimir-Bauer S, Lianidou ES. RASSF1A promoter methylation in high-grade serous ovarian cancer: A direct comparison study in primary tumors, adjacent morphologically tumor cell-free tissues and paired circulating tumor DNA. *Oncotarget*. 2017;8(13):21429-21443. doi:10.18632/oncotarget.15249
32. Díez-Villanueva, A., Mallona, I. & Peinado, M.A. Wanderer, an interactive viewer to explore DNA methylation and gene expression data in human cancer. *Epigenetics & Chromatin.* 2015; 8: 22. doi:10.1186/s13072-015-0014-8

33. Lambert S, Bennett V. Postmitotic expression of ankyrinR and beta R-spectrin in discrete neuronal populations of the rat brain. *J Neurosci*. 1993;13(9):3725-3735. doi:10.1523/JNEUROSCI.13-09-03725.1993

34. Bourguignon LY, Zhu H, Shao L, Zhu D, Chen YW. Rho-kinase (ROK) promotes CD44v(3,8-10)-ankyrin interaction and tumor cell migration in metastatic breast cancer cells. *Cell Motil Cytoskeleton*. 1999;43(4):269-287. doi:10.1002/(SICI)1097-0169(1999)43:4<269::AID-CM1>3.0.CO;2-5

35. Zhu D, Bourguignon LY. Interaction between CD44 and the repeat domain of ankyrin promotes hyaluronic acid-mediated ovarian tumor cell migration. *J Cell Physiol*. 2000;183(2):182-195. doi:10.1002/(SICI)1097-4652(200005)183:2<182::AID-JCP5>3.0.CO;2-O

36. Chen Y, Löhr M, Jesnowski R. Inhibition of ankyrin-B expression reduces growth and invasion of human pancreatic ductal adenocarcinoma. *Pancreatology*. 2010;10(5):586-596. doi:10.1159/000308821

37. Liao C, Huang X, Gong Y, Lin Q. Discovery of core genes in colorectal cancer by weighted gene co-expression network

analysis. *Oncol Lett*. 2019;18(3):3137-3149. doi:10.3892/ol.2019.10605

38. Stein L, Rothschild J, Luce J, et al. Copy number and gene expression alterations in radiation-induced papillary thyroid carcinoma from chernobyl pediatric patients. *Thyroid*. 2010;20(5):475-487. doi:10.1089/thy.2009.0008
39. Kiang KM, Leung GK. A Review on Adducin from Functional to Pathological Mechanisms: Future Direction in Cancer. Biomed Res Int. 2018 May 16;2018:3465929. doi: 10.1155/2018/3465929.
40. Luo C, Shen J. Adducin in tumorigenesis and metastasis. Oncotarget. 2017 Jul 18;8(29):48453-48459. doi: 10.18632/oncotarget.17173.
41. Ackermann A, Schrecker C, Bon D, Friedrichs N, Bankov K, Wild P, Plotz G, Zeuzem S, Herrmann E, Hansmann ML, Brieger A. Downregulation of SPTAN1 is related to MLH1 deficiency and metastasis in colorectal cancer. PLoS One. 2019 Mar 11;14(3):e0213411. doi: 10.1371/journal.pone.0213411.
42. Wu ZH, Zhou T, Sun HY. DNA methylation-based diagnostic and prognostic biomarkers of nasopharyngeal carcinoma patients. *Medicine (Baltimore)*. 2020;99(24):e20682. doi:10.1097/MD.0000000000020682

43. Heddleston JM, Li Z, Lathia JD, Bao S, Hjelmeland AB, Rich JN. Hypoxia inducible factors in cancer stem cells. *Br J Cancer*. 2010;102(5):789-795. doi:10.1038/sj.bjc.6605551

44. Lau KW, Tian YM, Raval RR, Ratcliffe PJ, Pugh CW. Target gene selectivity of hypoxia-inducible factor-alpha in renal cancer cells is conveyed by post-DNA-binding mechanisms. *Br J Cancer*. 2007;96(8):1284-1292. doi:10.1038/sj.bjc.6603675

45. Wallace EM, Rizzi JP, Han G, et al. A Small-Molecule Antagonist of HIF2α Is Efficacious in Preclinical Models of Renal Cell Carcinoma. *Cancer Res*. 2016;76(18):5491-5500. doi:10.1158/0008-5472.CAN-16-0473

46. Li Z, Bao S, Wu Q, et al. Hypoxia-inducible factors regulate tumorigenic capacity of glioma stem cells. *Cancer Cell*. 2009;15(6):501-513. doi:10.1016/j.ccr.2009.03.018

47. Sun HX, Xu Y, Yang XR, et al. Hypoxia inducible factor 2 alpha inhibits hepatocellular carcinoma growth through the transcription factor dimerization partner 3/ E2F transcription factor 1-dependent apoptotic pathway [published correction appears in Hepatology. 2018 Feb;67(2):808]. *Hepatology*. 2013;57(3):1088-1097. doi:10.1002/hep.26188

48. Imamura T, Kikuchi H, Herraiz MT, et al. HIF-1alpha and HIF-2alpha have divergent roles in colon cancer. *Int J Cancer*. 2009;124(4):763-771. doi:10.1002/ijc.24032

49. Rawłuszko-Wieczorek AA, Horbacka K, Krokowicz P, Misztal M, Jagodziński PP. Prognostic potential of DNA methylation and transcript levels of HIF1A and EPAS1 in colorectal cancer. *Mol Cancer Res*. 2014;12(8):1112-1127. doi:10.1158/1541-7786.MCR-14-0054

50. Westerlund I, Shi Y, Toskas K, et al. Combined epigenetic and differentiation-based treatment inhibits neuroblastoma tumor growth and links HIF2α to tumor suppression. *Proc Natl Acad Sci U S A*. 2017;114(30):E6137-E6146. doi:10.1073/pnas.1700655114

51. Klahan S, Wong HS, Tu SH, et al. Identification of genes and pathways related to lymphovascular invasion in breast cancer patients: A bioinformatics analysis of gene expression profiles. *Tumour Biol*. 2017;39(6):1010428317705573. doi:10.1177/1010428317705573

52. Fuady JH, Gutsche K, Santambrogio S, Varga Z, Hoogewijs D, Wenger RH. Estrogen-dependent downregulation of hypoxia-inducible factor (HIF)-2α in invasive breast cancer cells

[published correction appears in Oncotarget. 2017 Mar 21;8(12):20516]. *Oncotarget*. 2016;7(21):31153-31165. doi:10.18632/oncotarget.8866

53. Jarman EJ, Ward C, Turnbull AK, et al. HER2 regulates HIF-2α and drives an increased hypoxic response in breast cancer. *Breast Cancer Res*. 2019;21(1):10. Published 2019 Jan 22. doi:10.1186/s13058-019-1097-0

54. Huang J, Wang L. Cell-Free DNA Methylation Profiling Analysis-Technologies and Bioinformatics. *Cancers (Basel)*. 2019;11(11):1741. Published 2019 Nov 6. doi:10.3390/cancers11111741

55. Xu XH, Bao Y, Wang X, et al. Hypoxic-stabilized EPAS1 proteins transactivate DNMT1 and cause promoter hypermethylation and transcription inhibition of EPAS1 in non-small cell lung cancer [published online ahead of print, 2018 Jun 19]. *FASEB J*. 2018;fj201700715. doi:10.1096/fj.201700715

56. Pan R, Zhou C, Dai J, et al. Endothelial PAS domain protein 1 gene hypomethylation is associated with colorectal cancer in Han Chinese. *Exp Ther Med*. 2018;16(6):4983-4990. doi:10.3892/etm.2018.6856

57. Kent WJ, Sugnet CW, Furey TS, Roskin KM, Pringle TH, Zahler AM, Haussler D. The human genome browser at UCSC. Genome Res. 2002;12(6):996-1006

58. Győrffy B, Lanczky A, Eklund AC, Denkert C, Budczies J, Li Q, Szallasi Z. An online survival analysis tool to rapidly assess the effect of 22,277 genes on breast cancer prognosis using microarray data of 1,809 patients. Breast Cancer Res Treat. 2010 Oct;123(3):725-31. doi: 10.1007/s10549-009-0674-9

# 국문 초록

# 개의 유선암과 인간의 유방암 모두에서의 ANK2 의 과메틸화

요하네스 요세프스 스커보트

서울대학교 대학원 수의학과전공

지도교수 : 조제열, DVM, PhD

개의 유선암 (canine mammary gland tumor)은 사람 여성의 유방암과 같이 암컷 개에서 가장 흔히 발견되는 암이다. 개의 유선암과 사람의 유방암에 존재하는 여러 유사성 때문에 개의 유선암을 연구하는 것은 수의학에 국한된 것이 아니라 사람의 유방암을 이해하기 위한 비교의학적 측면에서 매우 중요하다. DNA 메틸화를 조직 및 액체생검에서 생체 표지자로 사용하는 시도는 많이 진행되고 있지만, 개의 유선암에 대한 연구는 매우 제한적으로 이루어지고 있다. 이 연구에서, 우리는 개의 유선암 조직의 메틸롬(Methylome) 분석을 통해 ANK2 및 EPAS 유전자의 인트론 영역에서 정상 조직과 다른 차등 메틸화 영역(Differentially methylated regions, DMGs)을 발견하였다. 또한, 이 두 지역의 차등 메틸화를 조직뿐만 아니라 환자유래 혈장에 존재하는 순환 유리 DNA (Cell free DNA, cfDNA)로부터 정량 할 수

있는 정량적 메틸화 특이적 PCR(quantitative methylation specific PCR, qMSP) 방법을 확립하였다. 이 방법을 통해 우리는 두 영역의 유선암 특이 과 메틸화를 추가된 조직 생검 시료를 통해 확인하였다. 나아가, ANK2 인트론 영역은 조직 생검 시료뿐만 아니라 유선암 환자 유래 혈장에 존재하는 cfDNA 에서도 유의한 메틸화를 보였다. 이 결과는 ANK2 및 EPAS 의 인트론 영역의 메틸화가 유선암의 조직은 물론 액체생검을 위한 생체표지자로 사용될 수 있음을 의미한다. 흥미롭게도, 우리는 이러한 ANK2 의 개유선암 특이 과메틸화는 비교 의학적인 측면에서 사람의 유방암에서도 과메틸화 되어있는 경향을 확인할 수 있었다. 이 연구 결과는 비교의학적 접근이 가지는 장점을 잘 보여주며, 이를 이용한 실제 임상적용을 위한 활용가능성을 높여준다.

**키워드** : 유선암; 비교 종양학; 과 메틸화; MSP; 바이오 마커; cfDNA; 유방암.

**학생 번호** : 2019-25838

# Hypermethylation of ANK2 on both Canine Mammary Tumors and Human Breast Cancer

Advisor: Professor Je-Yoel Cho

Submitting a master's thesis of
Veterinary Biochemistry

2020 November

Graduate School of Veterinary Medicine
Seoul National University
Veterinary Biomedical Science Major

Johannes Josephus Schabort

Confirming the master's thesis written by
Johannes Josephus Schabort
2020 December

Chair HANG LEE (Signature)

Vice Chair Je-Yoel Cho (Signature)

Examiner WAN HEE KIM (Signature)

Master's Thesis of Veterinary Biochemistry

# Hypermethylation of ANK2 on both Canine Mammary Tumors and Human Breast Cancer

## 개의 유선암과 인간의 유방암 모두에서의 ANK2 의 과 메틸화

2021 February

Graduate School of Veterinary Medicine

Seoul National University

Veterinary Biomedical Science Major

Johannes Josephus Schabort

# Hypermethylation of ANK2 on both Canine Mammary Tumors and Human Breast Cancer

Advisor: Professor Je-Yoel Cho

Submitting a master's thesis of
Veterinary Biochemistry

2020 November

Graduate School of Veterinary Medicine
Seoul National University
Veterinary Biomedical Science Major

Johannes Josephus Schabort

Confirming the master's thesis written by
Johannes Josephus Schabort
2020 December

Chair _____(Signature)

Vice Chair _____(Signature)

Examiner _____(Signature)

# Abstract

Canine Mammary Tumors (CMT) constitute the most common tumor types found in female dogs. Understanding this cancer through extensive research is important not only for clinical veterinary applications, but also in the scope of comparative oncology. The use of DNA methylation as a biomarker has been noted for numerous cancers in the form of both tissue and liquid biopsies, yet the study of methylation in CMT has been limited. By analyzing our canine Methyl-binding domain sequencing (MBD-seq) data, we identified intron regions of canine ANK2 and EPAS1 as differentially methylated regions (DMGs) in CMT. Subsequently, we established quantitative Methylation Specific PCR (qMSP) of ANK2 and EPAS1 to validate the target hypermethylation in CMT tissue, as well as cell free DNA (cfDNA) from CMT plasma. Both ANK2 and EPAS1 were hypermethylated in CMT and highlighted as potential tissue biomarkers in CMT. ANK2 additionally showed significant hypermethylation in the plasma cfDNA of CMT, indicating that it could be a potential liquid biopsy biomarker as well. A similar trend towards hypermethylation was indicated in HBC at a specific CpG of

the ANK2 target on the orthologous human region, which validates the comparative approach using aberrant methylation in CMT.

**Keywords:** CMT; comparative oncology; hypermethylation; MSP; biomarker.

**Student Number:** 2019-25838

---

# Table of Contents

Abstract……3

Table of Contents……5

List of Figures and Tables……7

1. Introduction……9

2. Results……12

2.1Identification of differentially methylated region

2.2Evaluation of differentially methylated regions in CMT and adjacent normal tissue

2.3Detection of differential methylation in canine plasma cfDNA

2.4Orthologous human regions analyzed from TCGA data

3. Discussion……33

4. Materials and Methods……41

4.1Ethics

4.2Tissue and plasma samples

4.3Correlation analysis between methylation and gene expression

4.4DNA isolation

4.5Bisulfite Sequencing

4.6Quantitative Methylation-Specific PCR (qMSP)

4.7Human TCGA Data

Bibliography……53

# List of Figures and Tables

**Figure 1.** Selection of ANK2 and EPAS1 as CMT hypermethylated targets.

**Figure 2.** BSP Sequencing of ANK2 and EPAS1.

**Figure 3.** QMSP validation of ANK2 and EPAS1 hypermethylation.

**Figure 4.** CMT hypermethylation analysis in cfDNA.

**Figure 5.** Hypermethylation of orthologous human target ANK2 and EPAS1 regions.

**Table 1.** Sequence homology of target canine ANK2 and EPAS1 regions with their orthologous human regions.

**Table 2.** Orthologous ANK2 region in other species.

**Table 3.** Canine tissue and plasma information.

**Table 4.** Human female breast cancer and normal plasma samples.

Table 5. Primer sets for BSP and MSP.

# 1. Introduction

Canine Mammary Tumors (CMT) are the most common neoplasia diagnosed in female dogs and are found to be malignant in approximately 50% of cases [1-4]. Apart from the clear veterinary benefit to understanding the nature of this cancer more clearly, studying CMT can also be beneficial in the field of comparative oncology [5-7].

Dogs have been highlighted as excellent animal models for human cancer [5,6]; this includes the use of CMT as a comparative model for human breast cancer (HBC) [7-10]. The expedited study rate due to faster disease progression and shorter lifespan, histological and mechanistic similarities [5], spontaneous disease occurrence, and exposure to similar environments as humans make dogs ideal models for comparative oncology [11,12]. The similar environments to humans that dogs often inhabit as companion animals are particularly interesting from an epigenetic standpoint, as environmental stimuli have been known to influence epigenetics [13, 14].

DNA methylation is an important method of epigenetic regulation and thus has often been studied in relation to cancer [15]. Aberrant global hypomethylation and localized, specific hypermethylation of

tumor suppressors and hypomethylation of oncogenes are observed in cancer [16]. In CMT, aberrant methylation has been reported for a few genes such as ERα [17], DAPK1, MGMT [18], and BRCA1[19], yet gene-specific methylation of CMT remains largely unknown. These methylation changes are often observed early during carcinogenesis [20] making them ideal biomarkers for early detection and prognosis. Tissue biomarkers still remain the standard for cancer diagnosis and prognosis, yet in recent years the interest in liquid biopsy biomarkers have risen [21].

Liquid biopsies involve the investigation of cell-free DNA (cfDNA) found in the blood, plasma, serum, or other liquids from the body and often contain circulating tumor DNA. They are of clinical importance as they are less invasive and also allow for a more comprehensive view of the cancer biology as opposed to the view offered by tissue biopsies that is limited to a single site of the tumor at a single moment in the progression of the cancer [21]. Methylation of circulating cfDNA has been highlighted as a human cancer biomarker in liquid biopsies [22-24]. Previously, our lab has presented the cfDNA hypomethylation of LINE1 as a candidate liquid biopsy biomarker in both CMT and HBC, however, the method of restriction enzyme

digestion followed by quantitative-PCR needs to be improved further for clinical use [25].

This study set out to identify and investigate differentially methylated regions (DMRs) in CMT, initially validating our findings in CMT tissues and then also in cfDNA isolated from plasma obtained from dogs with CMT with the intent of establishing candidate tissue and liquid biomarkers for cfDNA. Additionally, we correlated our differentially methylated target regions in our CMT data with HBC data to see if the differential methylation seen in these diseases is consistent across species at the targeted sites.

# 2. Results

## 2.1. Identification of differentially methylated regions

Target hypermethylated DMRs were identified using MBD-seq and corresponding RNA-seq according to the scheme in Figure 1A. From our previous MBD-seq data obtained for 11 pairs of CMT and adjacent normal tissue from NCBI BioProject database (accession number PRJNA601533)[26], 16,061 differentially methylated genes (DMGs) were identified based on the presence of a differentially methylated region (DMR) within the gene body. To develop DNA methylation-based biomarkers applicable to CMT and HBC, we decided to narrow the scope to regions that contained a hypermethylated CpG island in CMT; a separate study could be performed to analyze the hypomethylated cohort. We further narrowed down the 1,269 hypermethylated DMGs, based on the fold change (log2 fold change >1.5). Of these 20 identified targets, EPAS1, ANK2, DST and RUSC2 indicated a downregulation of gene expression in CMT noted from the RNA-seq data. Of these, ANK2 and EPAS1 were at a significant level (p-value <0.05) and were thus selected for further analysis (Figure 1B). These identified CMT DMRs were found in CpG islands in the 21$^{st}$ and 1$^{st}$ introns of ANK2 and

EPAS1, respectively, and the increase in methylation in the cancer samples are shown via Linear Mixed Model (LMM) with thresholds of both 10% and 5% (Figure 1C). The overall methylation level detected via the MBD-seq for both target regions were shown to be significantly more methylated in the CMT samples as opposed to the normal samples (Figure 1D).

Of the 11 CMT/normal tissue pairs that were used for MBD-seq, 10 were also used in the RNA-seq analysis. These 10 pairs that had data for both MBD-seq and RNA-seq showed a general reverse correlation trend between expression and methylation for both targets, albeit not at a significant level (Figure 1E & F). Yet, the correlation plots and the associated density plots do clearly reveal that for both targets the level of methylation is higher in CMT than in normal, whereas the level of expression is lower. Compared to the paired normal samples an increase in methylation of ANK2 and EPAS1 along with a decrease in expression is indicated in 5/10 and 8/10 CMT samples, respectively (Figure 1E & F). Based on the accumulated bioinformatic data, comprising MBD-seq and RNA-seq data, ANK2 and EPAS1 were both highlighted as potential CMT biomarkers with

DMRs in CMT and were chosen as the targets for the remainder of this study.

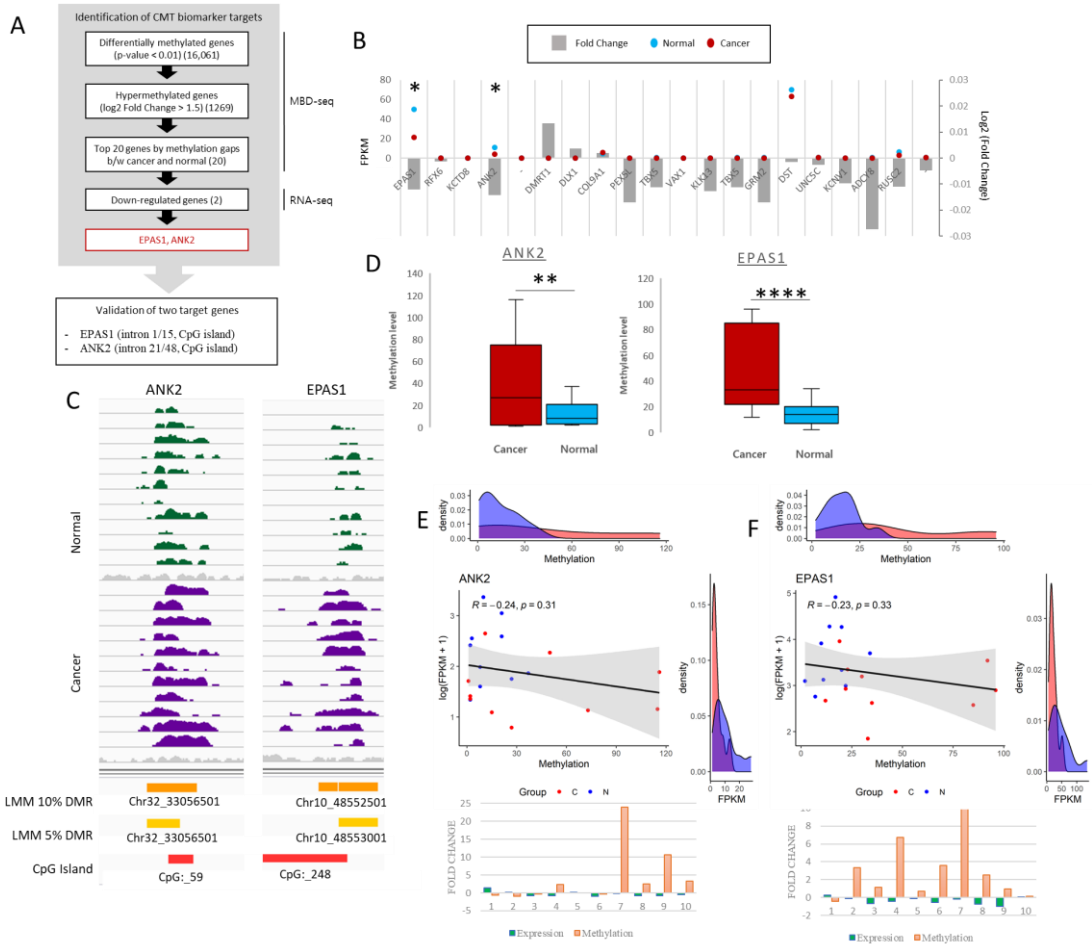


**Figure 1.** Selection of ANK2 and EPAS1 as CMT hypermethylated targets. (A) Schematic overview of target selection using MBD-seq and RNA-seq. (B) RNA-seq gene expression in FPKM of top 20 hypermethylated genes; blue dots=normal, red dots=CMT, * = p-value<0.05. Fold change (log2) for each target gene indicated with grey bar graph. (C) IGV peak calling for ANK2 and EPAS1 in both normal and cancer. Differential methylation assigned via LMM with both 5% and 10% threshold, and CpG island presence is indicated. (D)

Overall methylation levels of ANK2 and EPAS1 from MBD-seq data for 11 paired CMT and adjacent normal samples. EdgeR. ** = p.value<0.01, **** = <0.0001. (E) ANK2 and (F) EPAS1 correlation plots between expression (FPKM) and methylation of 10 paired CMT (red) and normal (blue) samples with matching density plots for both FPKM and methylation. Pearson correlation |r| value and p value indicated. Fold change graphs are also depicted for 10 CMT samples indicating expression (green) and methylation (orange).

## 2.2. Evaluation of differentially methylated regions in CMT and adjacent normal tissue

The target intron regions of ANK2 and EPAS1 that were identified through MBD-seq were further analyzed to assess their differential methylation. Quantitative Methylation Specific PCR (qMSP) was chosen as the method by which methylation was to be analyzed mainly due to its ability to quantify the methylation of numerous samples simultaneously without the need for exhaustive cloning and sequencing procedures. qMSP is furthermore a very sensitive technique that is able to distinguish a very small amount of methylated CpGs from unmethylated CpGs [27]. Sequencing was however still performed on three randomly selected pairs of CMT and normal gDNA for each target to establish a representative methylation pattern for each target and thus indicate in which areas to design the MSP primers (Figure 2). Both the ANK2 and EPAS1 target regions were methylated more in the CMT than the paired normal samples, although the amount of differential methylation was varied across the sample pairs (Figure 2).

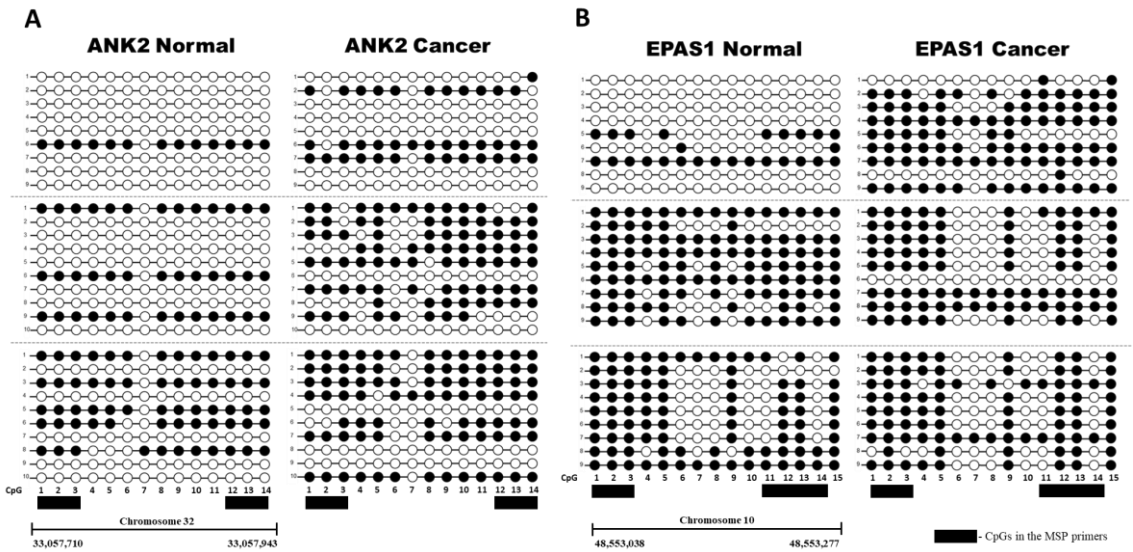


Figure 2. BSP Sequencing of ANK2 and EPAS1. Between 9 and 10 colonies were sequenced for three paired normal and CMT samples (separated by grey dotted line) for (A) ANK2 and (B) EPAS1. Methylation of a particular CpG is indicated by a black circle, and non-methylation is indicated by a white circle. The CpGs that were included in the forward and reverse MSP primers for each respective target with a black box.

qMSP was then performed to investigate more sample pairs. The Methylation Index is presented and is based on the Demethylation Index first introduced by Akirav et.al [28], with the adjustment of measuring the amount of methylated DNA as opposed to unmethylated DNA. This method uses bisulfite sequencing PCR (BSP) primers that flank the MSP region of interest to normalize the MSP readings (Figure 3A). Of the 15 sample pairs analyzed for the ANK2 target, 12 were more methylated in CMT compared to normal based on the methylation index, whereas 9 out of 15 EPAS1 target samples were more methylated in CMT than in paired normal (Figure 3B). The overall methylation was shown to be significantly more methylated in CMT for both the ANK2 and EPAS1 targets, based on paired t-tests (Figure 3C). Receiver Operating Characteristic (ROC) curves were constructed for both targets to access the sensitivity and specificity of using CMT hypermethylation as biomarkers. ANK2 had an Area under the curve (AUC) of 0.764, and EPAS1 had an AUC of 0.733 (Figure 3D). Overall, the quantitative MSP results validated what was shown in the MBD and sequencing data; the targeted ANK2 intron 21 and EPAS1 intron 1 regions are hypermethylated in CMT and are candidate tissue biomarkers for this disease.

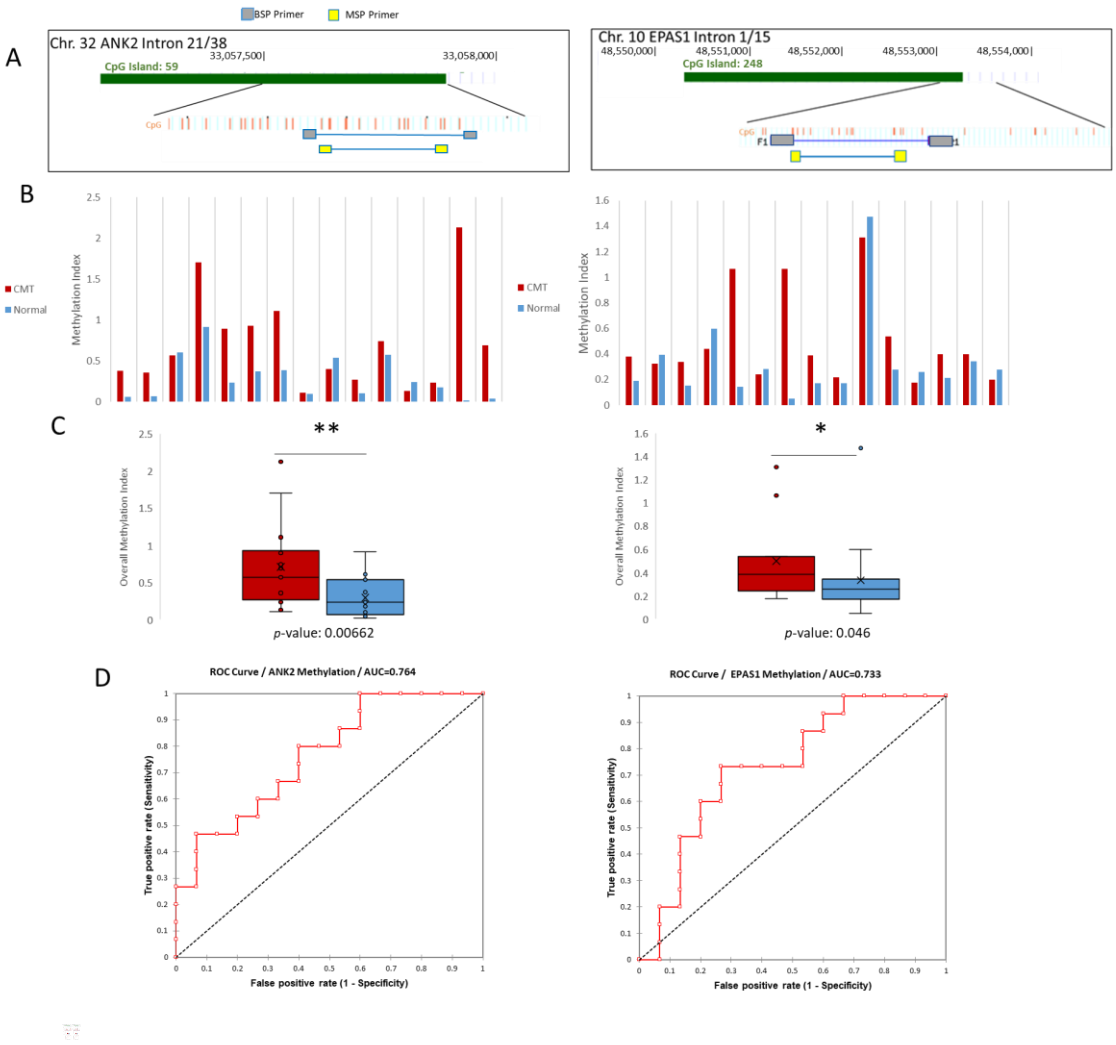


**Figure 3.** QMSP validation of ANK2 and EPAS1 hypermethylation. (A) Schemes for both ANK2 and EPAS1 indicating the target region in terms of its position on the CpG island of its respective intron. BSP primers (grey) are shown to flank the regions targeted by the MSP primers (yellow). (B) Methylation Indexes for both ANK2 and EPAS1. CMT samples are shown in red and paired

normal samples are shown in blue. (C) Overall methylation indexes for both ANK2 and EPAS1 are shown. CMT in red, normal in blue. * = p-value<0.05, ** = <0.01. (D) ROC curve analyses for ANK2 and EPAS1.

## 2.3 Detection of differential methylation in canine plasma cfDNA

qMSP has been utilized in previous studies to detect methylation of cfDNA [29,30]. One study found a significant agreement between ESR1 methylation of paired plasma and primary ovarian cancer tumors [31]. To evaluate whether the hypermethylation trends noted in CMT tissue could also be detected in cfDNA and thus serve as potential liquid biopsy biomarkers for CMT, we conducted the same qMSP procedure on cfDNA isolated from plasma samples of CMT and normal female dogs. The ANK2 target was analyzed in pooled cfDNA samples from 19 CMT dogs and 10 normal dogs. The hypermethylation trend of the ANK2 target region in CMT extended to cfDNA as is shown by the significantly higher methylation index (Fig 4A). Interestingly, the EPAS1 target, which was investigated in cfDNA samples from 10 CMT and 10 normal dogs, did not indicate an increased level of methylation for CMT as was seen in the tissue samples (Fig 4B). In contrast, the CMT cfDNA showed less methylation in CMT than normal plasma for EPAS1. Overall, in canine cfDNA, ANK2 demonstrated significant hypermethylation in CMT samples, which proposes it as a potential liquid biopsy biomarker for CMT.

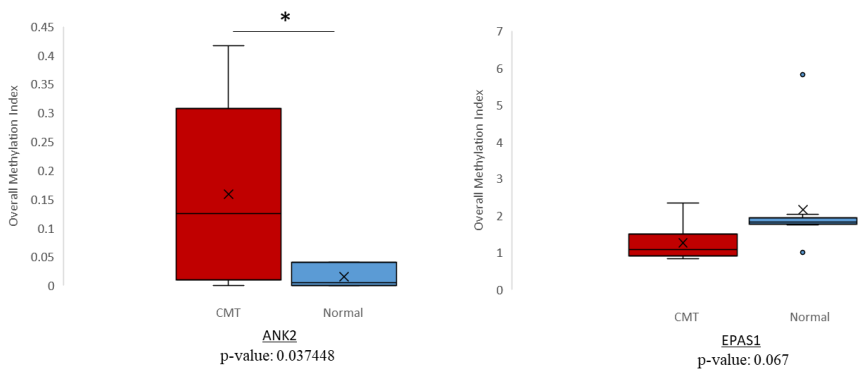


**Figure 4.** CMT hypermethylation analysis in cfDNA. Overall methylation index for (A) ANK2 and (B) EPAS1 in CMT (red) and normal (blue) cfDNA. * indicates p.value<0.05.

## 2.4. Orthologous human regions analyzed from TCGA data

To investigate whether the hypermethylation trend seen at the target regions in CMT would correspond to what is seen in HBC, we mapped the target regions found on the dog genome (CanFam3.1) to the human genome (HG19). This indicated that our 500 bp regions identified from the canine MBD-seq for the ANK2 and EPAS1 targets had orthologous human regions of 405 bp with 79% sequence identity and 221 bp with 76% sequence identity, respectively (Table 1). The EPAS1 target had an orthologous region that was also located in a CpG island at the 3' end of the first intron, just as in canines. The ANK2 target, which is situated in the 21$^{st}$ intron of the canine gene, similarly had an orthologous region in the 21$^{st}$ intron of human ANK2, however, this region does not contain a CpG island on the human genome, which makes it unsuitable for study with the qMSP method that we employed in this study. Even so, we investigated TCGA data for the target regions using Wanderer [32] and found ANK2 to be hypermethylated at 3 of the 4 CpG probes in this region (cg 25915539, cg17665652, and cg08448479), which corresponds to the hypermethylation that we observed in the orthologous region in dog (Fig 5A). Interestingly, even

though the amount of CpGs in this region is much less in humans than dogs, these three hypermethylated human CpGs are all conserved between the two species and were shown to be hypermethylated in the CMT dog samples (Fig 2A). The expression data from TCGA also indicated a downregulation of ANK2 in HBC, which matches our canine data (Fig 5B) and this data is further supported by the survival plot of ANK2 that shows a lower survival rate with decreased ANK2 expression (Fig 5C). The human EPAS1 region orthologous to the hypermethylated canine EPAS1 region that we analyzed contained 2 hypermethylated CpG probes according to the TCGA data (Fig 5D). Furthermore, the EPAS1 expression level was shown to be downregulated in HBC and the survival rate was decreased in accordance with EPAS1 downregulation (Fig 5E & F). The ANK2 target region, having been the better of the two targets, was furthermore investigated in additional species beyond canine and human. Mouse, rat, cat, and chimp all indicated orthologous intron regions with ≥74% identity conservation with the dog region (Table 2).

| | | % ID | Alignment length | Mismatches | Gaps open | e-value | bit-score |
|---|---|---|---|---|---|---|---|
| Canine ANK2 | Human ANK2 | | | | | | |
| chr32:33057501-33058000 | chr4:113292804-113293277 | 79.259 | 405 | 65 | 14 | 3.34E-75 | 265 |
| Canine EPAS1 | Human EPAS1 | | | | | | |
| chr10:48553001-48553500 | chr2:46299513-46300026 | 76.018 | 221 | 40 | 7 | 1.59E-37 | 141 |

Table 1. Sequence homology of target canine ANK2 and EPAS1 regions with their orthologous human regions.

| | Gene location | CpG Island | Regulatory Signatures | % ID | Alignment length | Gaps open | e-value | bit-score |
|---|---|---|---|---|---|---|---|---|
| Canine ANK2 | | | | | | | | |
| chr32:33057501-33058000 | Intron 21/48 | Yes | | | | | | |
| Human ANK2 | | | | | | | | |
| chr4:113292804-113293277 | Intron 19/43 | No | Proximal Enhancer-like | 79.259 | 405 | 14 | 3.34E-75 | 265 |
| Mouse ANK2 | | | | | | | | |
| chr3:126998115-126998598 | Intron 21/45 | No | Promotor-like | 74 | 423 | 26 | 3e-65 | 233 |
| Rat ANK2 | | | | | | | | |
| chr2:231301458-231301940 | Intron 19/21 | No | | 74 | 407 | 19 | 5e-63 | 224 |
| Cat ANK2 | | | | | | | | |
| chrB1:112372275-112372757 | Intron | Yes | | 82 | 501 | 19 | 3e-142 | 489 |
| Chimp ANK2 | | | | | | | | |
| chr4:110893204-110893679 | Intron | No | | 79 | 405 | 19 | 1e-95 | 334 |

Table 2. Orthologous ANK2 region in other species. Sequence homolgy information between dog and other species is indicated, along with the presence of CpG islands or other regulatory signatures.

To evaluate whether these trends would hold for clinical cfDNA samples, we isolated some from human plasma, obtained from both normal and HBC patients, and subjected it to bisulfite PCR sequencing. Unexpectedly, the EPAS1 target region did not show any methylation in this region for either HBC (4 samples) or normal (2 samples consisting of 5 and 6 pooled cfDNA isolates, respectively) (Data not shown), but this does coincide with the unexpected lack of cfDNA hypermethylation in CMT (Fig 4B). The hypermethylation trends shown in EPAS1 CMT tissue and HBC data from TCGA seems to not hold up in either canine or human cfDNA. On the other hand, sequencing results of the ANK2 target region from human cfDNA was more in line with what was suggested by the TCGA data. We sequenced colonies from 4 separate samples of HBC cfDNA and from 5 pooled normal cfDNA samples. Of the 3 CpGs indicated to be hypermethylated in this region from the TCGA data, only cg08448479, designated as CpG 5, was also shown to be more methylated in HBC cfDNA according to our sequencing results (Fig 5G). CpG 5 showed an increase in methylation from 71.88% in normal to 85.48% in HBC, which is consistent with the largest increase in methylation seen for the orthologous canine CpGs from 31.04% in normal to 62.07% in CMT (Fig 5G). We attempted to perform the qMSP procedure on pooled

samples of HBC cfDNA (14 samples) and pooled sample of normal human cfDNA (5 samples) with MSP primers that incorporated CpGs 1, 2, and 3 and CpGs 5 and 6 in the forward and reverse primers, respectively, but no significant difference was observed (Fig 5H). In both the TCGA dataset and the cfDNA sequencing, the ANK2 target indicated hypermethylation, even if limited to only a few CpGs, which is concurrent with what was seen in the canine CMT data.

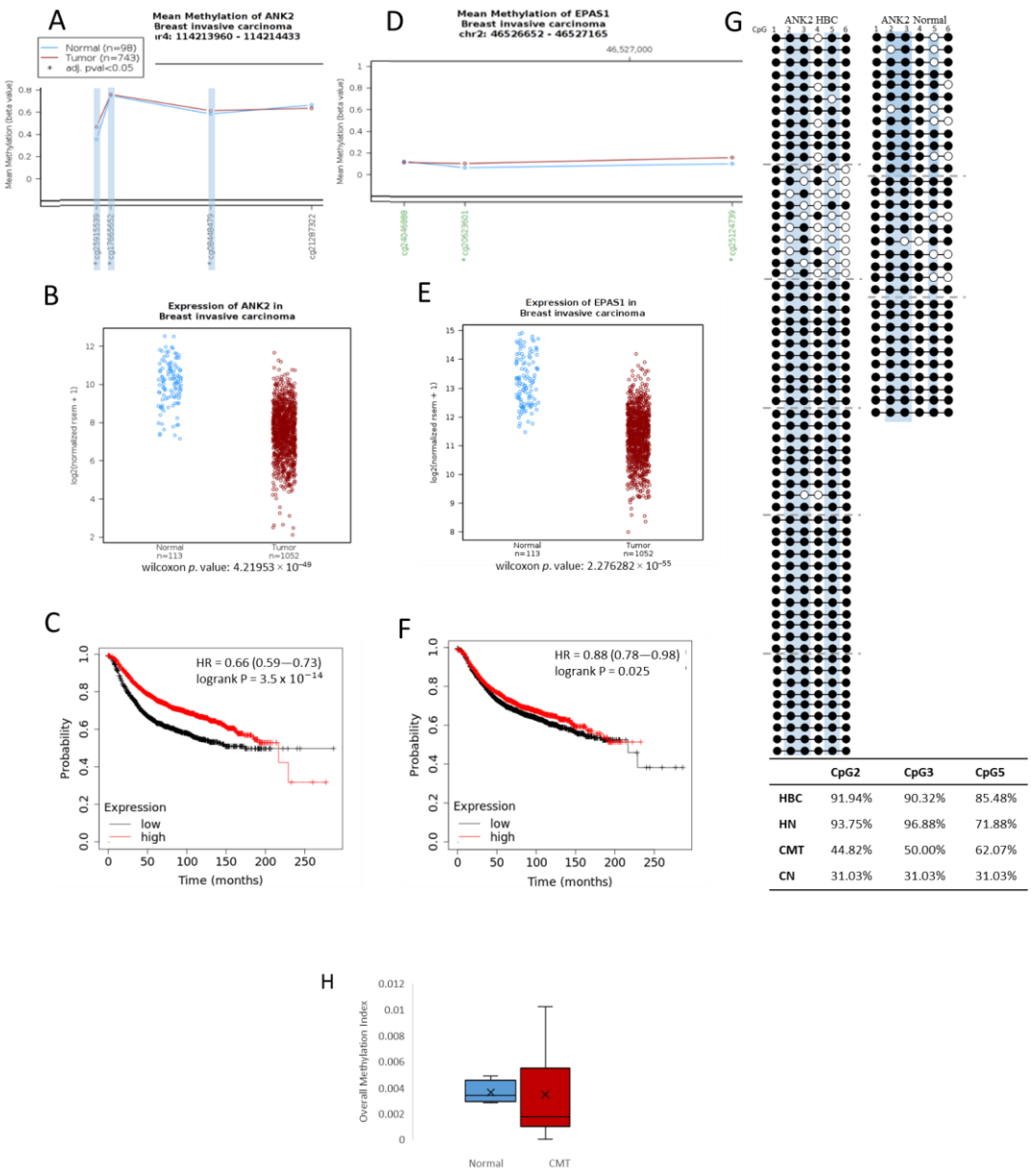


| | CpG2 | CpG3 | CpG5 |
|---|---|---|---|
| HBC | 91.94% | 90.32% | 85.48% |
| HN | 93.75% | 96.88% | 71.88% |
| CMT | 44.82% | 50.00% | 62.07% |
| CN | 31.03% | 31.03% | 31.03% |

**Figure 5.** Hypermethylation of orthologous human target ANK2 and EPAS1 regions. Mean Methylation (beta value) plots for orthologous human (A)ANK2 and (D)EPAS1 regions for normal

(blue) and invasive breast cancer patient(red) data obtained from TCGA. Specific methylation probes, annotated at the bottom of the graph are indicated to be in a CpG island when written in green ( only seen for EPAS1), and designated as significant (*) with an adjusted p-value <0.05. Three significantly hypermethylated CpGs from ANK2 are highlighted in light blue to indicate that they are conserved in the dog genome. (B) ANK2 and (E) EPAS1 log2 (normalized rsem + 1) expression data from TCGA for normal (blue) and invasive breast cancer patients (red). Wilcoxon p-values are indicated. (C) ANK2 and (F) EPAS1 Kaplan-Meier plots indicting relapse-free survival with high and low expressions each. (G) ANK2 sequencing results for cfDNA from normal and HBC patients. Between 10 and 11 colonies were sequenced for 6 individual HBC cfDNA samples (separated by grey dotted lines) and between 10 and 12 colonies were sequenced from 3 separate normal cfDNA samples. Methylation of a specific CpG is indicated by a black circle and non-methylation by a white circle. The CpGs at positions 2, 3, and 5 are highlighted in light blue as these are the CpGs that correlate with the hypermethylated CpG probes indicated in (A) and the respective percentage methylation for these CpGs in the HBC and

normal human (HN) cfDNA samples, as well as in canine CMT and normal (CN) tissue (Fig 2A), are indicated in the inserted table. (H) Overall Methylation Index for ANK2 in HBC and normal cfDNA.

# 3. Discussion

CMT is a common malignancy in female dogs and, moreover, in the scope of using dogs as animal models for human disease, its study can be translated to HBC. The field of comparative oncology using canine models have been increasing in popularity, yet the epigenome of canines with CMT remains incomplete. Methylation of DNA has been highlighted as a biomarker in both tissue and liquid biopsies [22-24] and thus we set out in this study to evaluate potential methylation biomarkers in CMT. This study identified novel regions in the 21$^{st}$ and 1$^{st}$ introns of ANK2 and EPAS1, respectively, that were significantly hypermethylated in CMT tissue and, in the case of ANK2, also in cfDNA isolated from dogs suffering from the disease. The ANK2 region was furthermore shown to be hypermethylated in human cfDNA at a corresponding CpG on the orthologous human region.

ANK2 encodes multiple AnkyrinB isoforms, which are integral membrane proteins that connect the lipid bilayer to the membrane skeleton [33]. In this present study, it was indicated that ANK2 mRNA expression was downregulated in CMT and also in HBC based on TCGA data. It is of note that other members of the ankyrin family, ANK1 and ANK3, have been shown to be overexpressed in multiple

human cancers including breast cancer [34,35], while ANK2 overexpression has been shown in pancreatic cancer where it contributed to the malignant phenotype [36]. However, other studies found that ANK2 gene expression was downregulated in colorectal cancer [37] and thyroid cancer [38], which corresponds to what we found in this study. The expression status and role of ANK2 seems to vary amongst cancer types, and further investigation in a larger variety of cancers is required to better understand its relationship to cancer. In cancers such as CMT and HBC, where ANK2 is downregulated, the role of its downregulation and the mechanisms by which its absence could aid in cancer progression remains unknown. Yet, knowing that the ANK2 protein is an integral membrane protein that connects the lipid bilayer to the membrane skeleton [33], it can be inferred that its downregulation would decrease the structural stability of the cell membrane making it more malleable. From this it can be hypothesized that the downregulation of ANK2 could promote the cancer phenotype by aiding in cellular dysplasia. The plasticity of the cellular membrane could further potentially promote metastasis by increasing cellular motility and migration as has been suggested with the downregulation of other membrane skeletal proteins [39-41]. Further study to confirm the role and mechanisms of downregulated

ANK2 in CMT and HBC is needed. Moreover, the role of cancer associated aberrant methylation in ANK2 remains largely unknown. One previous study compiled datasets for nasopharyngeal cancer and found ANK2 to be hypomethylated and upregulated, highlighting it as a potential biomarker for this cancer type [42]. Our study found a hypermethylated intron 21 region of ANK2, in both tissue and cfDNA, and it was highlighted as a potential tissue and liquid biopsy biomarker for CMT. Yet the impact of this specific methylation in CMT as well as the fuller extent of ANK2 methylation, on the promotor region for instance, remains unknown and should be studied further.

Of the other species that we investigated, cat showed the highest conservation of this ANK2 region at 82% identity and it was also the only other species that indicated a CpG island within this area suggesting that its regulation may be most similar, yet both human and mouse indicted regulatory signatures, which indicates this regions' potential importance in these species as well (Table 2). Unfortunately, of all these species, human is the only one with publicly available breast cancer/mammary gland cancer methylome data for this region. Mouse has some methylome data for this region, but not mammary gland specific and the only murine cancer methylome data is for colon

cancer, which did not show any differential methylation in this region. The orthologous human region does contain hypermethylated CpGs but outside of a CpG island which makes the qMSP method difficult, even more so when considering that of the 6 CpGs in the region only one seemed to be differentially methylated based on the sequencing data in Fig. 5G. The subsequent failure of the qMSP in distinguishing significantly between the HBC and Normal ANK2 is probably due to there only being 1 CpG (CpG 5) that is differentially methylated, and the technique is reliant on more than 1 CpG being differentially methylated. Additional sequencing of this region in more samples would be the best way to highlight the differential methylation in the respective CpGs. Other regions on ANK2 that contain conserved CpG islands could potentially be more successfully analyzed via the qMSP method and could potentially prove more influential in the downregulation of expression seen in Fig 5B. Pyrosequencing could be another alternative to pursue, as opposed to cloning and Sanger sequencing. We did not observe any methylation difference on the promoter region in our previous MBD-seq data [26]. This orthologous human region should be further studied in the future in tissue and cell culture to further investigate the nature and role of these hypermethylated CpGs play a significant role in HBC. To our

knowledge, no other study has yet to elucidate the state of ANK2 in either HBC or CMT, which makes our novel investigation of ANK2 in these diseases very insightful.

EPAS1, on the other hand, is relatively well studied in its relation to cancer, including breast cancer. EPAS1 is part of the Hypoxia Inducible Factor (HIF) family and plays an important role in the hypoxic response pathway which is often associated with tumorigenesis [43]. EPAS1 acts as a transcription factor in hypoxic conditions with many of its targets being known to contribute to carcinogenesis, such as VEGF and VEGF-R1 [43,44]. It has been highlighted as an oncogene in numerous cancer types [45, 46], however EPAS1 has also been described as tumor suppressive in various other cancer types including neuroblastoma, colon cancer, and hepatocellular carcinoma, and shown to reduce tumor growth and improve patient outcomes when overexpressed [47-50]. In breast cancer, the role and expression levels of EPAS1 have been indicated to be subtype specific. Klahan et. al [51] found EPAS1 to be a subtype specific lymphovascular invasion marker in ER- and HER2+ breast cancer. It has additionally been demonstrated that there is an estrogen dependent downregulation of EPAS1 in ER+ but not ER- HBC and

proposed EPAS1 as a negative prognostic marker in HER2 + invasive breast cancer, since overexpression of EPAS1 worsen the prognosis in HER2 and ER+ [52,53].

This present study indicated an overall downregulation of EPAS1 in CMT and in invasive HBC, yet the role of DNA methylation still remains unclear as, despite the indication of hypermethylation of the proposed region in the first intron of human EPAS1 shown in the TCGA data, the cfDNA analysis showed no methylation difference between normal and HBC patients. Similarly, the canine cfDNA data did not show any increased methylation in this region, however, significant hypermethylation was noted in CMT tissue compared to paired adjacent normal tissue. This discrepancy between the tissue methylation and cfDNA methylation could potentially be explained by a lesser abundance of circulating tumor DNA (ctDNA) compared to normal cfDNA isolated from the plasma samples used, seeing as even though tumors usually secrete for a larger amount of cfDNA in the plasma there is currently no ideal method for separating ctDNA from total cfDNA. ctDNA is furthermore highly fragmented which could hinder its detection [54]. Analyzing the methylation of the EPAS1 target region in circulating tumor cells (CTCs) could prove insightful. The hypermethylation and mRNA downregulation noted in the CMT

tissue is however concurrent with previous studies where EPAS1 has been shown to be hypermethylated in its promotor with downregulated mRNA expression in non-small cell lung cancer [55] and colon cancer [49]. Although a separate study showed EPAS1 to be hypomethylated in colon cancer [56]. In CMT tissue, our study of EPAS1 and its indications of hypermethylation in cancer as opposed to normal remains a novel and intriguing finding and highlights this target as a candidate tissue biomarker for CMT. Yet, future studies should endeavor to delve deeper into the methylation of the targeted intron region in HBC by analyzing tissue and cell culture samples. Elucidating the functional role of this hypermethylation in CMT and potentially HBC, specifically in ER+ subtypes that have previously indicated downregulation in HBC [52] and in HER2 subtypes where it has been implicated as a prognostic marker [53], is important to understanding the regulation of EPAS1 and its potential role in CMT and HBC.

Overall, this study set out to investigate CMT tissues and cfDNA isolated from plasma obtained from dogs with CMT for potential biomarkers and attempt to translate the findings to HBC by ways of comparative oncology. This study identified novel hypermethylated intron regions for ANK2 and EPAS1 that could potentially serve as tissue biomarkers for CMT. Furthermore, the ANK2 target also

showed hypermethylation in cfDNA isolated from CMT, which highlights it as a potential liquid biopsy biomarker for CMT. In HBC 1 CpG from the orthologous human ANK2 region likewise indicated a hypermethylated trend in cfDNA isolated from HBC patients, which emphasizes the link between CMT and HBC epigenetic regulation.

# 4. Materials and Methods

## 4.1. Ethics

This study, including the materials and methods, was reviewed and approved by the Seoul National University Institutional Review Board/Institutional Animal Care and Use Committee (IACUC# SNU-170602-1/IRB#SNU 16-10-063), Samsung Medical Center IRB (#SMC2016-07-129-015), and the Seoul Metropolitan Government - Seoul National University Boramae Medical Center IRB (#20161123/16-2016-99/121).

## 4.2. Tissue and plasma samples

Tissue samples used in this study consisted of surgically removed CMT tissue and paired adjacent normal tissue obtained from a variety of dog breeds. Tumors identified as carcinomas were selected, yet the selection was not subtype specific (simple, complex, and ductal carcinomas) seeing as the MBD-seq data (accession number PRJNA601533) [26] did not show any subtype specific differences in methylation patterns for our targets. Canine blood samples were taken from dogs diagnosed with mammary carcinoma and normal samples were obtained from healthy dogs without cancer. A detailed roster of

the dogs used can be found in Table 3. Depending on the dog size, 2 to 4 mL of blood was collected in Vacuette EDTA tubes (Greiner Bio-One, Kremsmunster, Austria).

| Sample | Type | Age | Breed | Histological Type |
|---|---|---|---|---|
| 1 | CMT and Adjacent Normal Tissue | 10 | Great Pyrenese | Complex |
| 2 | CMT and Adjacent Normal Tissue | 13 | Cocker Spaniel | Ductal |
| 3 | CMT and Adjacent Normal Tissue | 13 | Cocker Spaniel | Tubular |
| 4 | CMT and Adjacent Normal Tissue | 13 | Schnauzer | Complex/Ductal |
| 5 | CMT and Adjacent Normal Tissue | 11 | Dachshund | Complex |
| 6 | CMT and Adjacent Normal Tissue | 15 | Poodle | Mixed |
| 7 | CMT and Adjacent Normal Tissue | 10 | Dachshund | Complex/Ductal |
| 8 | CMT and Adjacent Normal Tissue | 6 | Maltese | Unknown |
| 9 | CMT and Adjacent Normal Tissue | 14 | Shih-tzu | Mixed |
| 10 | CMT and Adjacent Normal Tissue | 14 | Schnauzer | Complex |
| 11 | CMT and Adjacent Normal Tissue | 14 | Schnauzer | Complex |
| 12 | CMT and Adjacent Normal Tissue | 11 | Maltese | Complex |
| 13 | CMT and Adjacent Normal Tissue | 13 | Cocker Spaniel | Simple |
| 14 | CMT and Adjacent Normal Tissue | 17 | Yorkshire Terrier | Complex |
| 15 | CMT and Adjacent Normal Tissue | 10 | Shih-tzu | Complex |
| 16 | CMT and Adjacent Normal Tissue | 16 | Schnauzer | Tubular |
| 17 | CMT and Adjacent Normal Tissue | 14 | Poodle | Unknown |
| 18 | CMT and Adjacent Normal Tissue | 10 | Shih-tzu | Unknown |
| 19 | CMT and Adjacent Normal Tissue | 14 | Dachshund | Adenocarcinoma |
| 20 | CMT and Adjacent Normal Tissue | 3 | Dachshund | Complex |
| 21 | CMT and Adjacent Normal Tissue | 12 | Shih-tzu | Simple |
| 22 | CMT and Adjacent Normal Tissue | 10 | Beagle | Ductal |
| 13 | CMT Plasma | 13 | Cocker Spaniel | Simple |
| 23 | CMT Plasma | 14 | Cocker Spaniel | Unknown |
| 24 | CMT Plasma | 13 | Korean Jindo | Adenocarcinoma |
| 25 | CMT Plasma | 11 | Maltese | Complex |
| 26 | CMT Plasma | 13 | Mixed | Complex |
| 27 | CMT Plasma | 13 | Yorkshire Terrier | Unknown |
| 28 | CMT Plasma | 14 | Dachshund | Complex |
| 29 | CMT Plasma | 5 | Poodle | Simple |
| 30 | CMT Plasma | 14 | Poodle | Complex |
| 31 | CMT Plasma | 12 | Bichon Frise | Complex |
| 32 | CMT Plasma | 11 | Cavalier King Charles Spaniel | Adenocarcinoma |
| 33 | CMT Plasma | 16 | Shih-tzu | Unknown |
| 34 | CMT Plasma | 14 | Cocker Spaniel | Unknown |
| 35 | CMT Plasma | 15 | Shih-tzu | Unknown |
| 36 | CMT Plasma | 14 | Mixed | Adenocarcinoma |
| 37 | CMT Plasma | 16 | Mixed | Complex |
| 38 | CMT Plasma | 8 | Alaskan Malamute | Unknown |
| 39 | CMT Plasma | 16 | Mixed | Adenocarcinoma |
| 40 | CMT Plasma | 14 | Poodle | Adenocarcinoma |
| 41 | Healthy Canine Plasma | 10 | Schnauzer | |
| 42 | Healthy Canine Plasma | 12 | Schnauzer | |
| 43 | Healthy Canine Plasma | 3 | Pomeranian | |
| 44 | Healthy Canine Plasma | 8 | Maltese | |
| 45 | Healthy Canine Plasma | 13 | Weimaraner | |
| 46 | Healthy Canine Plasma | 7 | Maltese | |
| 47 | Healthy Canine Plasma | 2 | Bichon Frise | |
| 48 | Healthy Canine Plasma | 8 | Poodle | |
| 49 | Healthy Canine Plasma | 3 | Spitz | |
| 50 | Healthy Canine Plasma | 3 | Mixed | |

Table 3. Canine Tissue and Plasma Information. The sample type, age, breed, and histological type of CMT is indicated.

Human blood samples were obtained from Samsung Medical Center, Seoul. After written informed consent was given, 4 to 6 mL of human blood was obtained from HBC patients scheduled to undergo surgery and from healthy control subjects that indicated no breast abnormalities upon examination. A detailed roster of the human subjects can be found in Table 4.

Both canine and human plasma samples were separated from the whole blood immediately after blood collection. An equal volume of Ficoll-Paque PLUS (GE Healthcare, Orsay, France) was added to each blood sample and centrifuged for 30 min, at 500 g, 18 °C without brake. Plasma was collected from the supernatant and stored at -80℃ until use.

| ID | Status | Age | Stage | ER | PR | HER2 |
|---|---|---|---|---|---|---|
| BC005 | HBC | 35 | IIA | + | + | - |
| BC012 | HBC | 36 | IIA | + | + | Equivocal |
| BC013P | HBC | 40 | IB | - | - | - |
| BC018 | HBC | 55 | 0 | - | - | + |
| BC016 | HBC | 47 | IA | - | - | - |
| BC022 | HBC | 54 | 0 | + | + | - |
| BC023 | HBC | 48 | IA | + | + | - |
| BC032 | HBC | 44 | IIB | - | - | - |
| BC035 | HBC | 34 | IA | - | - | - |
| BC038P | HBC | 41 | IA | + | + | - |
| BC043P | HBC | 47 | IA | + | + | - |
| BC055P | HBC | 43 | IA | + | + | - |
| BC058P | HBC | 54 | IA | - | - | - |
| BC059P | HBC | 38 | 0 | - | - | + |
| BC060P | HBC | 42 | IIB | - | - | - |
| BB012P | Healthy | 48 | | | | |
| BB026 | Healthy | 28 | | | | |
| BB027 | Healthy | 30 | | | | |
| BB041 | Healthy | 40 | | | | |
| BB043 | Healthy | 36 | | | | |

Table 4. Human female breast cancer and healthy plasma samples. Sample ID, status, and age are indicated for all samples. HBC samples also indicate cancer stage as well as the presence of ER, PR, and HER2.

## 4.3. Correlation analysis between methylation and gene expression

We performed an integrative analysis of MBD-seq (accession number PRJNA601533) [26] and RNA-seq data (SRA accession number: SRR8741587-SRR8741602) [25] from 8 overlapped tissue samples to identify canine mammary gland DNA methylation markers. We first selected DMRs which are located in a CpG island on the gene body and examined the correlation between DNA methylation and gene expression for each sample. To inspect the impact of DNA methylation on the local regulation of gene expression, the Pearson correlation (r) was calculated between the read count for DMRs located in CpG regions and the expression values of the corresponding genes. Log (fpkm+ 1) values were used to avoid taking log0 in the case of there being 0 counts. $|r| > 0.3$ and an adjusted p-value $< 0.05$ were set as the cutoffs for a significant correlation.

## 4.4. DNA isolation

Genomic DNA was isolated from 25mg samples of paired CMT and adjacent normal tissues using the DNEasy Blood & Tissue kit (Qiagen, Hilden, Germany) according to the manufacturer's protocol. The

recovered gDNA was quantified using a nanodrop spectrophotometer. Circulating cfDNA was isolated from both human (Normal and Breast Cancer patients) and canine (Normal and CMT patients) plasma samples using the QIAamp Circulating Nucleic Acid Kit (Qiagen, Hilden, Germany) according to the manufacturer's instructions. In short, 500 uL of plasma was brought up to 1mL with PBS and lysed with proteinase K and Buffer ACL before being bound, washed, and eluted from QIAamp mini columns on a vacuum manifold. Recovered cfDNA was quantified with a Qubit 3.0 Fluorometer using the Qubit HS dsDNA Assay (Invitrogen, Waltham, USA), according to the manufacturer's protocol.

## 4.5. Bisulfite Sequencing

DNA samples were Bisulfite treated using the EZ DNA Methylation-Lightning kit (Zymo Research, Irvine, USA), according to the manufacturer's instructions. Bisulfite treated DNA was quantified using the Qubit ssDNA Assay on the Qubit 3.0 Fluorometer (Invitrogen, Waltham, USA). Paired samples were brought to equal concentrations by diluting with water as appropriate before qMSP was performed.

Randomly selected samples of Bisulfite treated gDNA was sequenced to ascertain what the general methylation patterns are for both the ANK2 and EPAS1 targets in both CMT and normal tissue. Bisulfite Sequencing PCR (BSP) was conducted using the BSP primers (Table 5) and HotStart Taq DNA Polymerase (Bioneer, Daejeon, South Korea). Successful amplification was validated via gel electrophoresis on 2.0% Agarose gels. PCR amplicons were purified using the MEGAquick-spin Plus Total Fragment DNA Purification kit (Intron Biotechnology, Seongnam, South Korea) according to the manufacturer's protocol. The amplicons were then ligated into pGEM T-Easy vector (Promega, Madison, USA) and transformed into competent E. coli cells via heat-shock at 45℃ for 45s and plated on LB Agar plates that had been treated with Ampicillin, X-Gal, and IPTG to allow for Blue/White screening of colonies. White colonies were picked and sent for Sanger sequencing (Macrogen, Seoul, South Korea). cfDNA from human samples, HBC and normal, were similarly subjected to BSP sequencing.

| | | Forward primer | Reverse primer | Product size (bp) | Anealing Temperature (℃) |
|---|---|---|---|---|---|
| **Canine** | ANK2 BSP | TGAGTTTTTGTATAGTTGTAGTTAAAT | CTACTCTTCTAATAAAAAACACTTAAC | 235 | 60 |
| | ANK2 MSP | AATTTGTTATCGAGTTTTTCGCGG | CGCTTTAACCCTAAAATAATCGAACG | 185 | 66 |
| | EPAS1 BSP | AGAAAATAAAATTATAGTTAGTTTTTTTGA | AAACTTTTCCCTATTCCCAAAT | 240 | 60.5 |
| | EPAS1 MSP | AGTTAGTTTTTTTGAGCGCGTTGCGG | AACCCGACGCAAAACCGCGA | 172 | 70 |
| **Human** | ANK2 BSP | GAGTATAGTAAGGGAGTTGTTAGT | CCATCTACTACAAATAAAATATTACCAT | 198 | 61 |
| | ANK2 MSP | CGGTGTAATTAAACGAATTGGGATTTC | CTACAAATAAAATATTACCATCGAAAACACG | 149 | 68 |
| | EPAS1 BSP | GGGAGGGAATTTGTGTATTTTAT | ATTTTTCCCCTACTCCCAAA | 182 | 60.5 |

Table 5. Primer sets for BSP and MSP.

## 4.6. Quantitative Methylation-Specific PCR (qMSP)

To investigate the methylation of both cancer and normal gDNA and cfDNA, quantitative MSP was performed on each sample with MSP primers (Table 5) using the CFX96 Real-time PCR Detection System (Bio-Rad Laboratories, Hercules, USA). The same samples were also subjected to quantitative PCR using the BSP primers (Table 5), which were designed to flank the region of interest, to normalize the MSP readings and allow for the calculation of the Methylation Index, which was based on the demethylation index first introduced by Akirav et.al [27]. Each qMSP reaction contained 0.5units Hotstart Taq DNA Polymerase (Bioneer, Daejeon, South Korea), 0.625mM MgCl2, 0.2mM dNTPs, 0.5X SYBER Green (Life Technologies, Carlsbad, USA) and 10pmol each of forward and reverse primers in a 20uL total volume. For the gDNA samples, 5-30ng of template DNA was added, whereas 120-1200pg was added for the cfDNA samples. Each sample was run in triplicate using both the MSP and BSP primer sets and the thermal cycler conditions were as follows: 95℃ for 15min, denaturation at 95℃ for 30s, annealing at Annealing Temperature (Table 5) for 30s, elongation at 72℃ for 30s and final elongation at 72℃ for 5min.

All primers were manually designed and checked using the OligoEvaluator™ webtool. MSP primers were designed with at least 6

CpGs included in the set of primers, and with at least one CpG located in the last 3 bases at the 3' ends of the primer. BSP primers were designed with at least 4 non-CpG C's included in the primer set. For canine primer optimization, there are not any universally methylated and unmethylated controls commercially available. In-house controls were thus made. In short, fully methylated canine controls were made by treating ~1ug of canine gDNA with MssI methyltransferase (New England Biolabs, Ipswich, USA) according to the manufacturer's protocol. Fully unmethylated DNA was made by performing PCR with primers that flank the region of interest. The resulting amplimers were thus devoid of any methylation and served as completely unmethylated control template. Human primers were optimized on fully methylated and fully unmethylated human HCT116 DKO DNA (Zymo Research, Irvine, USA).

## 4.7. Orthologous Species Data

Using liftOver [57], we were able to convert the canine (CanFam3.1) genome coordinates of the differentially methylated intron regions of ANK2 and EPAS1 that we identified from the MBD-seq data to their orthologous regions on the human (Hg38) mouse (mm10), rat (rn6), cat (felCAT8), and chimp (panTRO6)

genomes. BLAST (https://blast.ncbi.nlm.nih.gov) was used to align the nucleotide sequences and determine the amount of sequence homology.

HBC data for the ANK2 and EPAS1 intron targets was obtained using Wanderer [32], which utilizes 450k Infinium Chip methylation arrays and Illumina HISeq RNA-seq data from The Cancer Genome Atlas (TCGA). Survival plots were generated using Kaplan-Meier Plotter with the auto selected cutoff enabled, which utilizes the expression data for the genes of interest, ANK2 (202920_at) and EPAS1 (200878_at), and the relapse free survival data of 3951 patients obtained from the GEO database [58]. The Kaplan-Meier Plotter software groups expression into high or low according to the median expression and then uses a Kaplan-Meier Plot to compare the two groups [58].

# Bibliography


1. Moe L. Population-based incidence of mammary tumours in some dog breeds. *J Reprod Fertil Suppl*. 2001;57:439-443.
2. Sorenmo K. Canine mammary gland tumors. *Vet Clin North Am Small Anim Pract*. 2003;33(3):573-596. doi:10.1016/s0195-5616(03)00020-2
3. Salas Y, Márquez A, Diaz D, Romero L. Epidemiological Study of Mammary Tumors in Female Dogs Diagnosed during the Period 2002-2012: A Growing Animal Health Problem. *PLoS One*. 2015;10(5):e0127381. Published 2015 May 18. doi:10.1371/journal.pone.0127381
4. Sleeckx N, de Rooster H, Veldhuis Kroeze EJ, Van Ginneken C, Van Brantegem L. Canine mammary tumours, an overview. *Reprod Domest Anim*. 2011;46(6):1112-1131. doi:10.1111/j.1439-0531.2011.01816.x
5. Paoloni M, Khanna C. Translation of new cancer treatments from pet dogs to humans. *Nat Rev Cancer*. 2008;8(2):147-56.
6. Rowell JL, McCarthy DO, Alvarez CE. Dog models of naturally occurring cancer. Trends Mol Med. 2011;17(7):380-388. doi:10.1016/j.molmed.2011.02.004

7. Gray M, Meehan J, Martínez-Pérez C, et al. Naturally-Occurring Canine Mammary Tumors as a Translational Model for Human Breast Cancer. *Front Oncol*. 2020;10:617. Published 2020 Apr 28. doi:10.3389/fonc.2020.00617
8. Strandberg JD, Goodman DG. Animal model of human disease: canine mammary neoplasia. *Am J Pathol*. 1974;75(1):225-228.
9. Visan S, Balacescu O, Berindan-Neagoe I, Catoi C. In vitro comparative models for canine and human breast cancers. *Clujul Med*. 2016;89(1):38-49. doi:10.15386/cjmed-519
10. Abdelmegeed SM, Mohammed S. Canine mammary tumors as a model for human disease. *Oncol Lett*. 2018;15(6):8195-8205. doi:10.3892/ol.2018.8411
11. Bukowski JA, Wartenberg D, Goldschmidt M. Environmental causes for sinonasal cancers in pet dogs, and their usefulness as sentinels of indoor cancer risk. *J Toxicol Environ Health A*. 1998;54(7):579-591. doi:10.1080/009841098158719
12. Lin CH, Lo PY, Wu HD, Chang C, Wang LC. Association between indoor air pollution and respiratory disease in companion dogs and cats. *J Vet Intern Med*. 2018;32(3):1259-1267. doi:10.1111/jvim.15143

13. Bollati V, Baccarelli A. Environmental epigenetics. Heredity (Edinb). 2010 Jul;105(1):105-12. doi: 10.1038/hdy.2010.2. Epub 2010 Feb 24. PMID: 20179736; PMCID: PMC3133724.

14. Baccarelli A, Bollati V. Epigenetics and environmental chemicals. Curr Opin Pediatr. 2009 Apr;21(2):243-51. doi: 10.1097/mop.0b013e32832925cc. PMID: 19663042; PMCID: PMC3035853.

15. Pfeifer GP. Defining Driver DNA Methylation Changes in Human Cancer. *Int J Mol Sci*. 2018;19(4):1166. Published 2018 Apr 12. doi:10.3390/ijms19041166

16. Baylin SB, Jones PA. Epigenetic Determinants of Cancer. *Cold Spring Harb Perspect Biol*. 2016;8(9):a019505. Published 2016 Sep 1. doi:10.1101/cshperspect.a019505

17. Brandão YO, Toledo MB, Chequin A, et al. DNA Methylation Status of the Estrogen Receptor α Gene in Canine Mammary Tumors. *Vet Pathol*. 2018;55(4):510-516. doi:10.1177/0300985818763711

18. Ren X, Li H, Song X, Wu Y, Liu Y. 5-Azacytidine treatment induces demethylation of *DAPK1* and *MGMT* genes and inhibits growth in canine mammary gland tumor cells. *Onco Targets Ther*.

2018;11:2805-2813. Published 2018 May 15.
doi:10.2147/OTT.S162381

19. Qiu H, Lin D. Roles of DNA mutation in the coding region and DNA methylation in the 5' flanking region of BRCA1 in canine mammary tumors. *J Vet Med Sci*. 2016;78(6):943-949.
doi:10.1292/jvms.15-0557

20. Feinberg, A., Ohlsson, R. & Henikoff, S. The epigenetic progenitor origin of human cancer. *Nat Rev Genet.* 2006;**7**:21-33.
doi:10.1038/nrg1748

21. Perakis S, Speicher MR. Emerging concepts in liquid biopsies. *BMC Med*. 2017;15(1):75. Published 2017 Apr 6.
doi:10.1186/s12916-017-0840-6

22. Board, R. E., Knight, L., Greystoke, A., Blackhall, F. H., Hughes, A., Dive, C., & Ranson, M. DNA Methylation in Circulating Tumour DNA as a Biomarker for Cancer. *Biomarker Insights*. 2007
doi:10.1177/117727190700200003

23. Huang J, Wang L. Cell-Free DNA Methylation Profiling Analysis-Technologies and Bioinformatics. *Cancers (Basel)*. 2019;11(11):1741. Published 2019 Nov 6.
doi:10.3390/cancers11111741

24. Constâncio V, Nunes SP, Henrique R, Jerónimo C. DNA Methylation-Based Testing in Liquid Biopsies as Detection and Prognostic Biomarkers for the Four Major Cancer Types. *Cells*. 2020;9(3):624. Published 2020 Mar 5. doi:10.3390/cells9030624

25. Lee KH, Shin TJ, Kim WH, Cho JY. Methylation of LINE-1 in cell-free DNA serves as a liquid biopsy biomarker for human breast cancers and dog mammary tumors [published correction appears in Sci Rep. 2019 Nov 20;9(1):17459]. *Sci Rep*. 2019;9(1):175. Published 2019 Jan 17. doi:10.1038/s41598-018-36470-5

26. Nam, A., Lee, K., Hwang, H. *et al.* Alternative methylation of intron motifs is associated with cancer-related gene expression in both canine mammary tumor and human breast cancer. *Clin Epigenet.* 2020;12:110. doi10.1186/s13148-020-00888-4

27. Herman JG, Graff JR, Myöhänen S, Nelkin BD, Baylin SB. Methylation-specific PCR: a novel PCR assay for methylation status of CpG islands. *Proc Natl Acad Sci U S A*. 1996;93(18):9821-9826. doi:10.1073/pnas.93.18.9821

28. Akirav EM, Lebastchi J, Galvan EM, et al. Detection of β cell death in diabetes using differentially methylated circulating DNA. *Proc*

*Natl Acad Sci U S A*. 2011;108(47):19018-19023. doi:10.1073/pnas.1111008108

29. Eissa MAL, Lerner L, Abdelfatah E, et al. Promoter methylation of ADAMTS1 and BNC1 as potential biomarkers for early detection of pancreatic cancer in blood. *Clin Epigenetics*. 2019;11(1):59. Published 2019 Apr 5. doi:10.1186/s13148-019-0650-0
30. Giannopoulou L, Mastoraki S, Buderath P, et al. ESR1 methylation in primary tumors and paired circulating tumor DNA of patients with high-grade serous ovarian cancer. *Gynecol Oncol*. 2018;150(2):355-360. doi:10.1016/j.ygyno.2018.05.026
31. Giannopoulou L, Chebouti I, Pavlakis K, Kasimir-Bauer S, Lianidou ES. RASSF1A promoter methylation in high-grade serous ovarian cancer: A direct comparison study in primary tumors, adjacent morphologically tumor cell-free tissues and paired circulating tumor DNA. *Oncotarget*. 2017;8(13):21429-21443. doi:10.18632/oncotarget.15249
32. Díez-Villanueva, A., Mallona, I. & Peinado, M.A. Wanderer, an interactive viewer to explore DNA methylation and gene expression data in human cancer. *Epigenetics & Chromatin.* 2015; 8: 22. doi:10.1186/s13072-015-0014-8

33. Lambert S, Bennett V. Postmitotic expression of ankyrinR and beta R-spectrin in discrete neuronal populations of the rat brain. *J Neurosci*. 1993;13(9):3725-3735. doi:10.1523/JNEUROSCI.13-09-03725.1993

34. Bourguignon LY, Zhu H, Shao L, Zhu D, Chen YW. Rho-kinase (ROK) promotes CD44v(3,8-10)-ankyrin interaction and tumor cell migration in metastatic breast cancer cells. *Cell Motil Cytoskeleton*. 1999;43(4):269-287. doi:10.1002/(SICI)1097-0169(1999)43:4<269::AID-CM1>3.0.CO;2-5

35. Zhu D, Bourguignon LY. Interaction between CD44 and the repeat domain of ankyrin promotes hyaluronic acid-mediated ovarian tumor cell migration. *J Cell Physiol*. 2000;183(2):182-195. doi:10.1002/(SICI)1097-4652(200005)183:2<182::AID-JCP5>3.0.CO;2-O

36. Chen Y, Löhr M, Jesnowski R. Inhibition of ankyrin-B expression reduces growth and invasion of human pancreatic ductal adenocarcinoma. *Pancreatology*. 2010;10(5):586-596. doi:10.1159/000308821

37. Liao C, Huang X, Gong Y, Lin Q. Discovery of core genes in colorectal cancer by weighted gene co-expression network

analysis. *Oncol Lett*. 2019;18(3):3137-3149. doi:10.3892/ol.2019.10605

38. Stein L, Rothschild J, Luce J, et al. Copy number and gene expression alterations in radiation-induced papillary thyroid carcinoma from chernobyl pediatric patients. *Thyroid*. 2010;20(5):475-487. doi:10.1089/thy.2009.0008
39. Kiang KM, Leung GK. A Review on Adducin from Functional to Pathological Mechanisms: Future Direction in Cancer. Biomed Res Int. 2018 May 16;2018:3465929. doi: 10.1155/2018/3465929.
40. Luo C, Shen J. Adducin in tumorigenesis and metastasis. Oncotarget. 2017 Jul 18;8(29):48453-48459. doi: 10.18632/oncotarget.17173.
41. Ackermann A, Schrecker C, Bon D, Friedrichs N, Bankov K, Wild P, Plotz G, Zeuzem S, Herrmann E, Hansmann ML, Brieger A. Downregulation of SPTAN1 is related to MLH1 deficiency and metastasis in colorectal cancer. PLoS One. 2019 Mar 11;14(3):e0213411. doi: 10.1371/journal.pone.0213411.
42. Wu ZH, Zhou T, Sun HY. DNA methylation-based diagnostic and prognostic biomarkers of nasopharyngeal carcinoma patients. *Medicine (Baltimore)*. 2020;99(24):e20682. doi:10.1097/MD.0000000000020682

43. Heddleston JM, Li Z, Lathia JD, Bao S, Hjelmeland AB, Rich JN. Hypoxia inducible factors in cancer stem cells. *Br J Cancer*. 2010;102(5):789-795. doi:10.1038/sj.bjc.6605551

44. Lau KW, Tian YM, Raval RR, Ratcliffe PJ, Pugh CW. Target gene selectivity of hypoxia-inducible factor-alpha in renal cancer cells is conveyed by post-DNA-binding mechanisms. *Br J Cancer*. 2007;96(8):1284-1292. doi:10.1038/sj.bjc.6603675

45. Wallace EM, Rizzi JP, Han G, et al. A Small-Molecule Antagonist of HIF2α Is Efficacious in Preclinical Models of Renal Cell Carcinoma. *Cancer Res*. 2016;76(18):5491-5500. doi:10.1158/0008-5472.CAN-16-0473

46. Li Z, Bao S, Wu Q, et al. Hypoxia-inducible factors regulate tumorigenic capacity of glioma stem cells. *Cancer Cell*. 2009;15(6):501-513. doi:10.1016/j.ccr.2009.03.018

47. Sun HX, Xu Y, Yang XR, et al. Hypoxia inducible factor 2 alpha inhibits hepatocellular carcinoma growth through the transcription factor dimerization partner 3/ E2F transcription factor 1-dependent apoptotic pathway [published correction appears in Hepatology. 2018 Feb;67(2):808]. *Hepatology*. 2013;57(3):1088-1097. doi:10.1002/hep.26188

48. Imamura T, Kikuchi H, Herraiz MT, et al. HIF-1alpha and HIF-2alpha have divergent roles in colon cancer. *Int J Cancer*. 2009;124(4):763-771. doi:10.1002/ijc.24032

49. Rawłuszko-Wieczorek AA, Horbacka K, Krokowicz P, Misztal M, Jagodziński PP. Prognostic potential of DNA methylation and transcript levels of HIF1A and EPAS1 in colorectal cancer. *Mol Cancer Res*. 2014;12(8):1112-1127. doi:10.1158/1541-7786.MCR-14-0054

50. Westerlund I, Shi Y, Toskas K, et al. Combined epigenetic and differentiation-based treatment inhibits neuroblastoma tumor growth and links HIF2α to tumor suppression. *Proc Natl Acad Sci U S A*. 2017;114(30):E6137-E6146. doi:10.1073/pnas.1700655114

51. Klahan S, Wong HS, Tu SH, et al. Identification of genes and pathways related to lymphovascular invasion in breast cancer patients: A bioinformatics analysis of gene expression profiles. *Tumour Biol*. 2017;39(6):1010428317705573. doi:10.1177/1010428317705573

52. Fuady JH, Gutsche K, Santambrogio S, Varga Z, Hoogewijs D, Wenger RH. Estrogen-dependent downregulation of hypoxia-inducible factor (HIF)-2α in invasive breast cancer cells

[published correction appears in Oncotarget. 2017 Mar 21;8(12):20516]. *Oncotarget*. 2016;7(21):31153-31165. doi:10.18632/oncotarget.8866

53. Jarman EJ, Ward C, Turnbull AK, et al. HER2 regulates HIF-2α and drives an increased hypoxic response in breast cancer. *Breast Cancer Res*. 2019;21(1):10. Published 2019 Jan 22. doi:10.1186/s13058-019-1097-0

54. Huang J, Wang L. Cell-Free DNA Methylation Profiling Analysis-Technologies and Bioinformatics. *Cancers (Basel)*. 2019;11(11):1741. Published 2019 Nov 6. doi:10.3390/cancers11111741

55. Xu XH, Bao Y, Wang X, et al. Hypoxic-stabilized EPAS1 proteins transactivate DNMT1 and cause promoter hypermethylation and transcription inhibition of EPAS1 in non-small cell lung cancer [published online ahead of print, 2018 Jun 19]. *FASEB J*. 2018;fj201700715. doi:10.1096/fj.201700715

56. Pan R, Zhou C, Dai J, et al. Endothelial PAS domain protein 1 gene hypomethylation is associated with colorectal cancer in Han Chinese. *Exp Ther Med*. 2018;16(6):4983-4990. doi:10.3892/etm.2018.6856

57. Kent WJ, Sugnet CW, Furey TS, Roskin KM, Pringle TH, Zahler AM, Haussler D. The human genome browser at UCSC. Genome Res. 2002;12(6):996-1006

58. Győrffy B, Lanczky A, Eklund AC, Denkert C, Budczies J, Li Q, Szallasi Z. An online survival analysis tool to rapidly assess the effect of 22,277 genes on breast cancer prognosis using microarray data of 1,809 patients. Breast Cancer Res Treat. 2010 Oct;123(3):725-31. doi: 10.1007/s10549-009-0674-9

# 국문 초록

# 개의 유선암과 인간의 유방암 모두에서의 ANK2 의 과메틸화

요하네스 요세프스 스커보트

서울대학교 대학원 수의학과전공

지도교수 : 조제열, DVM, PhD

개의 유선암 (canine mammary gland tumor)은 사람 여성의 유방암과 같이 암컷 개에서 가장 흔히 발견되는 암이다. 개의 유선암과 사람의 유방암에 존재하는 여러 유사성 때문에 개의 유선암을 연구하는 것은 수의학에 국한된 것이 아니라 사람의 유방암을 이해하기 위한 비교의학적 측면에서 매우 중요하다. DNA 메틸화를 조직 및 액체생검에서 생체 표지자로 사용하는 시도는 많이 진행되고 있지만, 개의 유선암에 대한 연구는 매우 제한적으로 이루어지고 있다. 이 연구에서, 우리는 개의 유선암 조직의 메틸롬(Methylome) 분석을 통해 ANK2 및 EPAS 유전자의 인트론 영역에서 정상 조직과 다른 차등 메틸화 영역(Differentially methylated regions, DMGs)을 발견하였다. 또한, 이 두 지역의 차등 메틸화를 조직뿐만 아니라 환자유래 혈장에 존재하는 순환 유리 DNA (Cell free DNA, cfDNA)로부터 정량 할 수

있는 정량적 메틸화 특이적 PCR(quantitative methylation specific PCR, qMSP) 방법을 확립하였다. 이 방법을 통해 우리는 두 영역의 유선암 특이 과 메틸화를 추가된 조직 생검 시료를 통해 확인하였다. 나아가, ANK2 인트론 영역은 조직 생검 시료뿐만 아니라 유선암 환자 유래 혈장에 존재하는 cfDNA 에서도 유의한 메틸화를 보였다. 이 결과는 ANK2 및 EPAS 의 인트론 영역의 메틸화가 유선암의 조직은 물론 액체생검을 위한 생체표지자로 사용될 수 있음을 의미한다. 흥미롭게도, 우리는 이러한 ANK2 의 개유선암 특이 과메틸화는 비교 의학적인 측면에서 사람의 유방암에서도 과메틸화 되어있는 경향을 확인할 수 있었다. 이 연구 결과는 비교의학적 접근이 가지는 장점을 잘 보여주며, 이를 이용한 실제 임상적용을 위한 활용가능성을 높여준다.

**키워드** : 유선암; 비교 종양학; 과 메틸화; MSP; 바이오 마커; cfDNA; 유방암.

**학생 번호** : 2019-25838